Electronic Supplementary Material (ESI) for Inorganic Chemistry Frontiers.

Coordination-Driven Supramolecular Syntheses of New Homo- and Hetero- polymetallic Cu(I) Assemblies : Solid-State and Solution Characterization

Ali Moustafa Khalil,[a] Chendong Xu,[a] Vincent Delmas,[a] Guillaume Calvez,[a] Karine Costuas,[a] Mohamed Haouas*[b] and Christophe Lescop*[a]

[a] Univ Rennes, INSA Rennes, CNRS, ISCR (Institut des Sciences Chimiques de Rennes) – UMR 6226, F-35000 Rennes, France. E-mail: christophe.lescop@insa-rennes.

[b] Institut Lavoisier de Versailles, UMR 8180 CNRS, UVSQ, Université Paris-Saclay, Versailles, France

Supporting Information

Table of contents

I. Experimental Section

For the syntheses reported, procedures were performed under air, in a simple flask. Commercially available solvents were used as received without further purification. Commercially available reagents ($[Cu(CH_3CN)_4]PF_6$, KCN and dppm, were obtained from Sigma-Aldrich. NaN3 and $Zn(NO_3)_2.6H_2O$ were supplied by Acros Organics. Sodium dicyanamide was obtained from TCI. $Cu(NO_3)_2{\cdot}3H_2O$ and $Cd(NO_3)_2{\cdot}4H_2O$ was supplied, respectively, by Fluka Chemika and Rectapur® Prolabo. The precursor **A** was synthesized according to a previously reported procedure.[S1]

All solution NMR spectra were measured in CD_2Cl_2 on a Bruker Avance 400 spectrometer using 5 mm standard NMR tubes. All ^{31}P and ^{1}H spectra, including 2D DOSY and *J*-Resolved, were recorded with decoupling from either ^{31}P or ^{1}H during acquisition at a Larmor frequency of 400.13 MHz for ^{1}H and 161.97 MHz for ^{31}P. Hahn echo pulse sequence with a pulse duration of 8 μs for 90° flip angle, 4 s recycle delay, 1 s acquisition time, and 16 number of scans, was used to record the 1D $^{1}H\{^{31}P\}$ spectra. Translational diffusion measurements were performed using Bruker's "ledbpgs2s" stimulated echo DOSY pulse sequence including bipolar and spoil gradients. Apparent diffusion coefficients were obtained using an adapted algorithm based on the inverse Laplace transform stabilized by maximum entropy. [S2] 2D *J*-Resolved experiment was recorded with standard Bruker pulse sequence employing 5 ms increment in t_1 dimension. $^{31}P\{^{1}H\}$ spectra were measured with a pulse duration of 16 μs (90° flip angle), 30 s recycle delay, 1 s acquisition time, and 32 number of scans. ^{113}Cd NMR spectrum was recorded at 88.78 MHz Larmor frequency using 18 μs (90° flip angle), 20 s recycle delay, 0.3 s acquisition time, and ca. 16000 number of scans. Chemical shifts are reported relative to tetramethylsilane (TMS) for ^{1}H, 85 wt.% H_3PO_4 for ^{31}P, and $CdMe_2$ for ^{113}Cd. Spectral deconvolution was done with DMFIT software (Version 2010).[S3]

FT-IR measurements have been performed on a Perkin Elmer Frontier spectrometer using UATR (Universal Attenuated Total Reflectance) accessory. Spectra have been recorded between 650 cm^{-1} and 4000 cm^{-1}, on pure samples.

UV-vis solid-state absorption measurements have been recorded on a Perkin-Elmer Lambda 650 spectrometer using a 60 mm integrating sphere. Spectra have been recorded between 800 nm and 200 nm, on pellets.

Steady-state emission spectra and luminescence quantum yield measurements were recorded on a *Horiba Jobin-Yvon* (*HJY*) Fluorolog-3 (FL3-2iHR550) fluorescence spectrofluorometer equipped with an IR R928P PMT / *HJY* FL-1073 detector and with an integrating sphere. Low temperature measurements were allowed by

using a OptistatCF (*Oxford Inst.*) in the range of 77 K to 300 K. Excited-state lifetimes in the range of 80 K to 300 K were measured with a delta hub (TCSPC: Time-Correlated-Single-Photon-Counting) + delta diode system allowing to measure excited-state lifetimes between 500 ps et 10 µs and with a pulsed xenon source (FL-1035) allowing to measure excited-state lifetimes longer than 10 µs.

Solid sample was placed in a quartz sample holders inside the integrating sphere and the cryostat and maintained at the desired temperature until equilibrium was reached before recording the spectrum.

The experimental data were then fitted according to the following equation [S4]

$$\tau(\mathrm{obs}) = \frac{1 + \frac{1}{3}\exp(-\frac{\Delta E_{\mathrm{ST}}}{k_{\mathrm{B}}T})}{\frac{1}{\tau(\mathrm{T_1})} + \frac{1}{3\tau(\mathrm{S_1})}\exp(-\frac{\Delta E_{\mathrm{ST}}}{k_{\mathrm{B}}T})} \qquad \text{equation (S1)}$$

where τ(obs), $\tau(S_1)$, $\tau(T_1)$, k_B, T and ΔE_{ST} represent the observed lifetime, singlet state decay lifetime, triplet state decay lifetime, Boltzmann constant, temperature and singlet-triplet energy difference, respectively.

Powder X-ray diffraction diagrams have been collected using a Panalytical X'Pert Pro diffractometer with an X'celerator detector. The typical recording conditions were 45 kV, 40 mA for Cu Kα (λ = 1.542Å), the diagrams were recorded in theta/theta mode in 60 min between 5° and 50° with a step size of 0.0084° and a scan time of 50 s.

Synthesis of derivative D

To a dichloromethane solution (10 ml) of the derivative **A** (0.04 g, 0.018 mmol) was added a methanol suspension (5 ml) of $NaN(CN)_2$ (0.0016 g, 0.018 mmol). This reaction mixture was stirred overnight at room temperature along the appearance of few amount of white precipitate. This crude solution was then filtered over cotton and was after left upon pentane vapor diffusion, affording the derivative **D** (0.052 g, 0.012 mmol, 68 % yield) as an air-stable colorless solid.

^{1}H NMR (400 MHz, CD_2Cl_2, ppm, figure S1): δ = 2.73 (broad d, 8H, PCH_2P), 3.54 (broad d, 8H, PCH_2P), 6.57 (broad s, 32H, H_{arom}), 6.81 (broad s, 24H, H_{arom}), 6.81 (broad s, 24H, H_{arom}), 7.05 (broad m, 32H, H_{arom}), 7.15 (broad s, 16H, H_{arom}), 7.60(broad s, 16H, H_{arom})., 7.68 (broad s, 16H, H_{arom}).

^{31}P{^{1}H} NMR (162 MHz, CD_2Cl_2, ppm, figure S2): δ = -13.8 (broad s, P_{dppm}), -14.4 (broad s, P_{dppm}), -15.2 (broad s, P_{dppm}), -16.08 (broad s, P_{dppm}), -16.8 to -20.0 (broad m, P_{dppm}), -143.5.5 (sept, PF_6^-, ^{1}J(P-F) = 713.0 Hz).

$^{13}C\{^{1}H\}$ NMR (100.6 MHz, CD_2Cl_2, ppm, figure S3): δ = 27.2 (bs, CH_2), 27.4 (bs, CH_2), 128.9 (s, Carom), 129.3 (bs, Carom), 130.0 (s, Carom), 131.1 (s, Carom), 133.3 (bs, Carom), 134.9 (bs, Carom), 136.2 (bs, Carom), 137.3 (bs, Carom), 154.8 (bs, C_{CN}).

IR (cm^{-1} figure S4): 690 (vw), 736 (w), 772 (m), 835 (vw), 998 (s), 1026 (s), 1095 (m), 1435 (m), 1484 (m), 1585 (vs), 2117 (υ(C≡N), w), 2144 (υ(DCM, s), 2205 (υ(DCM, w), 2285 (υ(DCM), m), 3051 (w).

Elemental analysis, calcd. (%) for $C_{211}H_{182}Cl_6Cu_8F_{12}N_{10}P_{18}$: C 58.07, H 4.20, N 3.21; found: C 58.46, H 4.12, N 3.02.

Synthesis of derivative E

A solution of the derivative **A** (50 mg, 0.023 mmol) in 15 ml dichloromethane was stirred 30 min at room temperature. To this suspension, a methanol solution (4 ml) of NaN_3 (3 mg, 0.046 mmol) was added. This reaction mixture was stirred 2 hours at room temperature. This crude solution was then filtered over cotton and was after left upon n-pentane vapour diffusion, affording the derivative **E** as tiny colourless needles. The derivative **E** sample was collected upon filtration and dried under air on paper affording a white crystalline powder in a yield of 69 % (70 mg, 0.032 mmol).

For NMR experiments aimed to characterize in solution this 1D-CP that partially dissociates in oligomeric fragments in solution, see table S1 and Figure S15. These ill resolved spectra results indicate that, although poorly soluble, this polymer dissociate partially and can be found in solution as small fragments of various nuclearities, very likely involved in multiple self-dissociation/re-organisation equilibria.

IR (cm^{-1}, figure S5): 683(vs), 734(s), 784(s), 843(vw), 913(vw), 995(w), 1026(w), 1094(m), 1186(w), 1327(w), 1434(s), 1482(m), 1574(w), 2045(υ(N_3), s), 2124(υ(C≡N), w), 3051(w).

Elemental analysis, calcd. (%) for $C_{52}H_{46}Cl_2Cu_2N_4P_4$: C 59.55, H 4.42, N 5.34; found: C 59.77, H 4.07, N 5.55.

Synthesis of derivatives F_{Cu}

To a dichloromethane solution (15 ml) of the derivative **A** (50 mg, 0.024 mmol) was added a methanol solution (4 ml) of sodium azide (3.3 mg, 0.050 mmol). The resulting colorless mixture was left upon stirring at

room temperature and under air for 5 min then an acetone solution (4 ml) of $Cu(NO_3)_2.3H_2O$ (2.8 mg, 0.011 mmol) was added. The color of the solution instantaneously turned to deep blue. The resulting clear reaction mixture was stirred 1 hour at room temperature, then precipitated with the addition of 20 ml of pentane, affording after filtration and drying the derivative $\mathbf{F_{Cu}}$ (42 mg, 0.071 mmol, 85 % yield) as an air-stable dark blue crystalline powder.

IR (cm^{-1}, figure S6): 690 (vs), 735 (vs), 783 (s), 837 (s), 999 (w), 1026 (w), 1096 (m), 1188 (vw), 1351 (w), 1435 (vs), 1483 (m), 1586 (vw), 1625 (vw), 2054 (υ_{N3}, vs), 2126 (υ_{CN}, w), 3053 (vw).

Elemental analysis, calcd. (%) for $C_{206}H_{180}Cl_4Cu_9F_{12}N_{16}P_{18}$: C 56.50, H 4.14, N 5.12; found: C 56.03, H 4.32, N 5.26.

Synthesis of derivative $\mathbf{F_{Zn}}$

To a dichloromethane solution (20 ml) of the derivative **A** (100 mg, 0.047 mmol) was added a methanol solution (5 ml) of sodium azide (6 mg, 0.09 mmol). The resulting colorless mixture was left upon stirring at room temperature under air for 5 min then an acetone solution (5 ml) of $Zn(NO_3)_2.6H_2O$ (6 mg, 0.023 mmol) was added. The resulting clear and colorless reaction mixture was stirred 1 hour at room temperature, then precipitated with the addition of 30 ml of pentane, affording after filtration and drying the derivative $\mathbf{F_{Zn}}$ (90 mg, 0.021 mmol, 91 % yield) as an air-stable colorless crystalline powder.

^1H NMR (400 MHz, CD_2Cl_2, ppm, figure S1): δ = 2.53 to 2.71 (m, 8H, PCH_2P), 3.38 to 3.56 (m, 8H, PCH_2P), 5.90 to 6.07 (broad m, 16H, H_{arom}), 6.61 (broad s, 8H, H_{arom}), 6.67 to 6.79 (broad m, 16H, H_{arom}), 6.88 to 7.03 (broad m, 64H, H_{arom}), 7.05 to 7.30 (broad m, 24H, H_{arom}), 7.45 (broad s, 16H, H_{arom}), 7.94 (broad s, 16H, H_{arom}).

$^{31}P\{^1H\}$ NMR (162 MHz, CD_2Cl_2, ppm, figure S2): δ = -13.8 (broad s, Pdppm), -14.1 (broad s, Pdppm), -14.6 (broad s, Pdppm), -14.8 (broad s, Pdppm), -15.2 (broad s, Pdppm), -17.3(broad s, Pdppm) , -17.7 (broad s, Pdppm) , -18.3 (broad s, Pdppm), -143.5 (sept, PF_6^-, $^1J(P\text{-}F)$ = 713.0 Hz).

$^{13}C\{^1H\}$ NMR (100.6 MHz, CD_2Cl_2, , ppm, figure S7): δ = 25.6 (bs, CH_2), 25.9 (bs, CH_2), 128.6 (s, Carom), 129.1 (s, Carom), 129.5 (s, Carom), 129.8 (s, Carom), 130.1 (s, Carom), 130.6 (s, Carom), 131.2 (bs, Carom), 133.9 (bs, Carom), 135.8 (bs, Carom), 136.6 (bs, Carom), 153.6 (bs, C_{CN}).

IR (cm^{-1}, figure S8): 689 (vs), 734 (vs), 782 (s), 835 (vs), 1000 (vw), 1026 (vw), 1096 (s), 1187 (vw), 1349 (vw), 1435 (s), 1483 (m), 1585 (vw), 2068 (υ_{N3}, vs), 2131 (υ_{CN}, w), 3053 (vw).

Elemental analysis, calcd. (%) for $C_{206}H_{180}Cl_4Cu_8Zn_1F_{12}N_{16}P_{18}$: C 56.48, H 4.14, N 5.12; found: C 56.12, H 4.57, N 5.29.

ESI-MS (CH_2Cl_2): m/z = measured 4057.3312 (1 ppm) $\mathbf{[F_{Zn}^{++}, PF_6^-]^+}$ ($C_{204}H_{176}N_{16}F_6P_{17}{}^{63}Cu_8{}^{64}Zn)^+$, calcd 4057.3367 **;** measured 1956.1844 (1 ppm) $\mathbf{[F_{Zn}]^{++}}$ ($C_{204}H_{176}N_{16}P_{16}{}^{63}Cu_8{}^{64}Zn)^{++}$, calcd 1956.1862.

Synthesis of derivative $\mathbf{F_{Cd}}$

To a dichloromethane solution (20 ml) of the derivative **A** (100 mg, 0.047 mmol) was added a methanol solution (5 ml) of sodium azide (6 mg, 0.09 mmol). The resulting colorless mixture was left upon stirring at room temperature under air for 5 min then an acetone solution (5 ml) of $Cd(NO_3)_2.4H_2O$ (7 mg, 0.023 mmol) was added. The resulting clear and colorless reaction mixture was stirred 1 hour at room temperature, then precipitated with the addition of 30 ml of pentane, affording after filtration and drying the derivative $\mathbf{F_{Cd}}$ (88 mg, 0.020 mmol, 88 % yield) as an air-stable colorless crystalline powder.

^{1}H NMR (400 MHz, CD_2Cl_2, ppm, figure S1): δ = 2.63 (bs, 8H, PCH_2P), 3.34 to 3.59 (m, 8H, PCH_2P), 6.01 (broad s, 16H, H_{arom}), 6.47 to 7.71 (broad m, 128H, H_{arom}), 7.90 (broad s, 16H, H_{arom}).

^{31}P{^{1}H} NMR (162 MHz, CD_2Cl_2, ppm, figure S2): δ = -14.0 to -16.4 (broad m, Pdppm), -17.0 to -19.3 (broad s, Pdppm), -143.5 (sept, PF_6^-, ^{1}J(P-F) = 713.0 Hz).

^{13}C{^{1}H} NMR (100.6 MHz, CD_2Cl_2, ppm, figure S9): δ = 26.1 (bs, CH_2), 128.7 (bs, Carom), 129.2 (s, Carom), 129.7 (bs, Carom), 130.2 (bs, Carom), 130.7 (s, Carom), 134.0 (bs, Carom), 135.7 (bs, Carom), 136.6 (bs, Carom), 154.0 (bs, C_{CN}).

^{113}Cd NMR (88.78 MHz, CD_2Cl_2, ppm, figure S10): δ = -350.2.

IR (cm^{-1}, figure S11): 691 (vs), 735 (vs), 785 (s), 834 (s), 999 (w), 1026 (w), 1095 (m), 1190 (vw), 1346 (vw), 1435 (s), 1483 (m), 1588 (vw), 1629 (vw), 2057 (υ_{N3}, vs), 2128 (υ_{CN}, w), 3051 (vw).

Elemental analysis, calcd. (%) for $C_{207}H_{182}Cl_6Cu_8Cd_1F_{12}N_{16}P_{18}$: C 55.09, H 4.06, N 4.97; found: C 54.85, H 4.11, N 5.06.

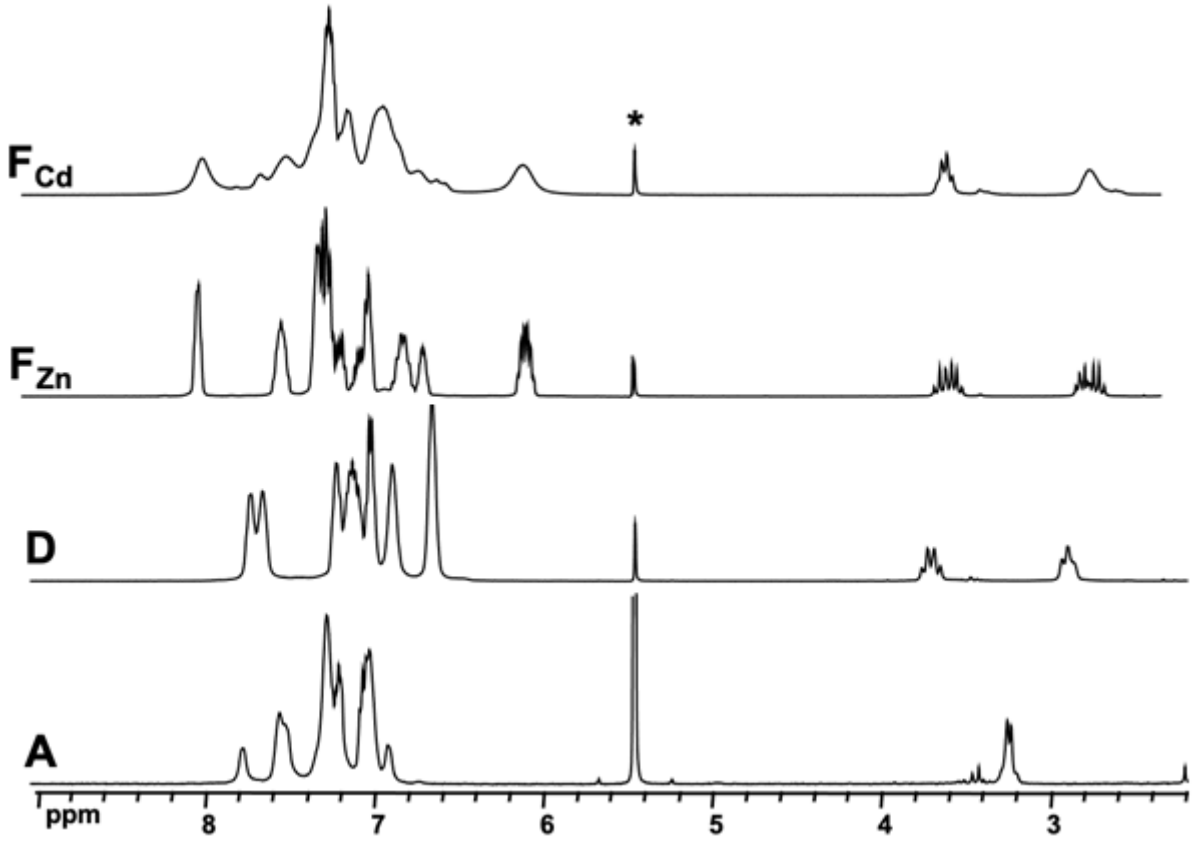

Figure S1. $^{1}H\{^{31}P\}$ NMR RT spectra of the precursor **A** and the derivatives **D**, $\mathbf{F}_{Zn}$, and $\mathbf{F}_{Cd}$ in CD_2Cl_2. Note the splitting of the CH_2 signal of dppm ligand at ca. 3.2 ppm in **A** into two resonances at ca. 2.8 and 3.7 ppm, indicating that these two protons become inequivalent in the supramolecular complexes **D**, $\mathbf{F}_{Zn}$, and $\mathbf{F}_{Cd}$. This may indicate that the structure of **A** in solution is highly fluxional on solution while those of the derivatives **D**, $\mathbf{F}_{Zn}$, and $\mathbf{F}_{Cd}$ are rigid, without dissociation in solution. Asterisk (*) denotes solvent signal.

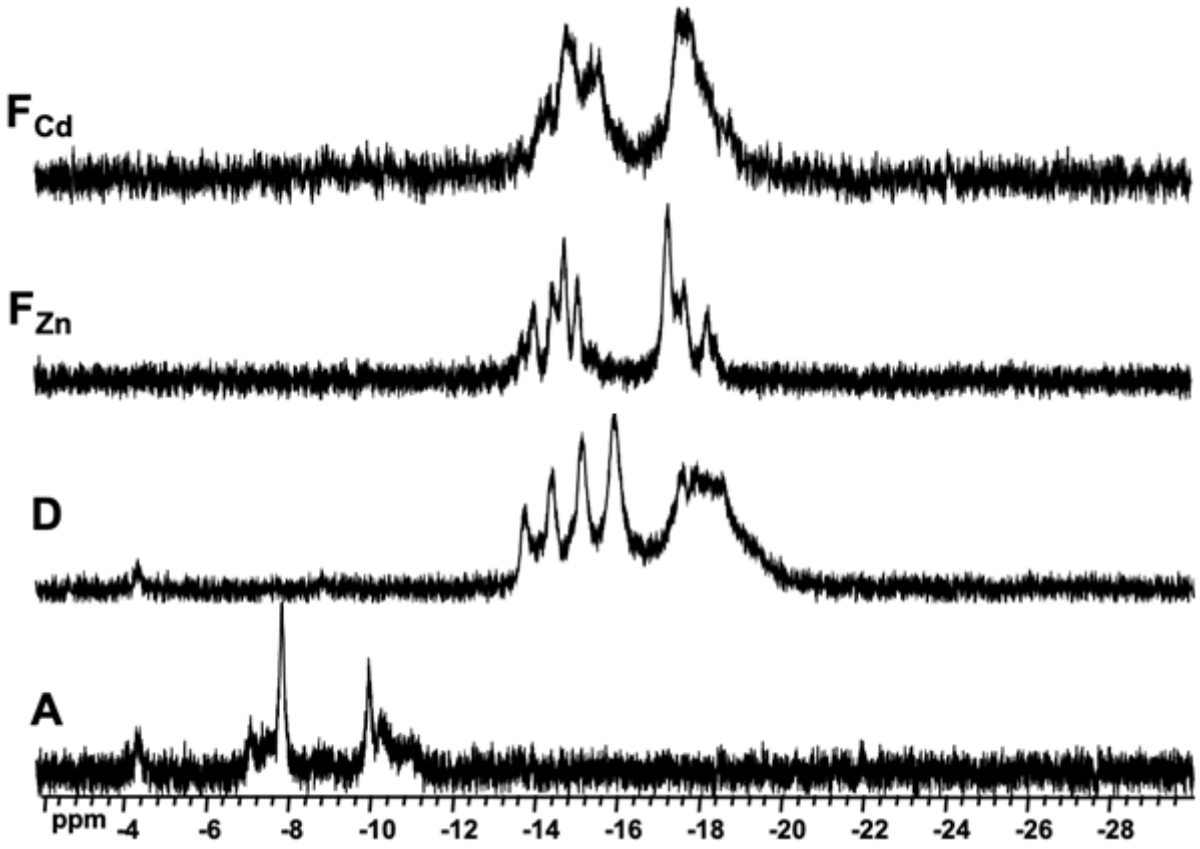

Figure S2. $^{31}P\{^{1}H\}$ NMR RT spectra of the precursor **A** and the derivatives **D**, $\mathbf{F}_{Zn}$, and $\mathbf{F}_{Cd}$ in CD_2Cl_2. Note the high field shifts of the signals in **D**, $\mathbf{F}_{Zn}$, and $\mathbf{F}_{Cd}$ by comparison to those in **A,** highlighting the similarity in the environment of dppm ligands in **D**, $\mathbf{F}_{Zn}$, and $\mathbf{F}_{Cd}$ and their significant differences with that present in **A**.

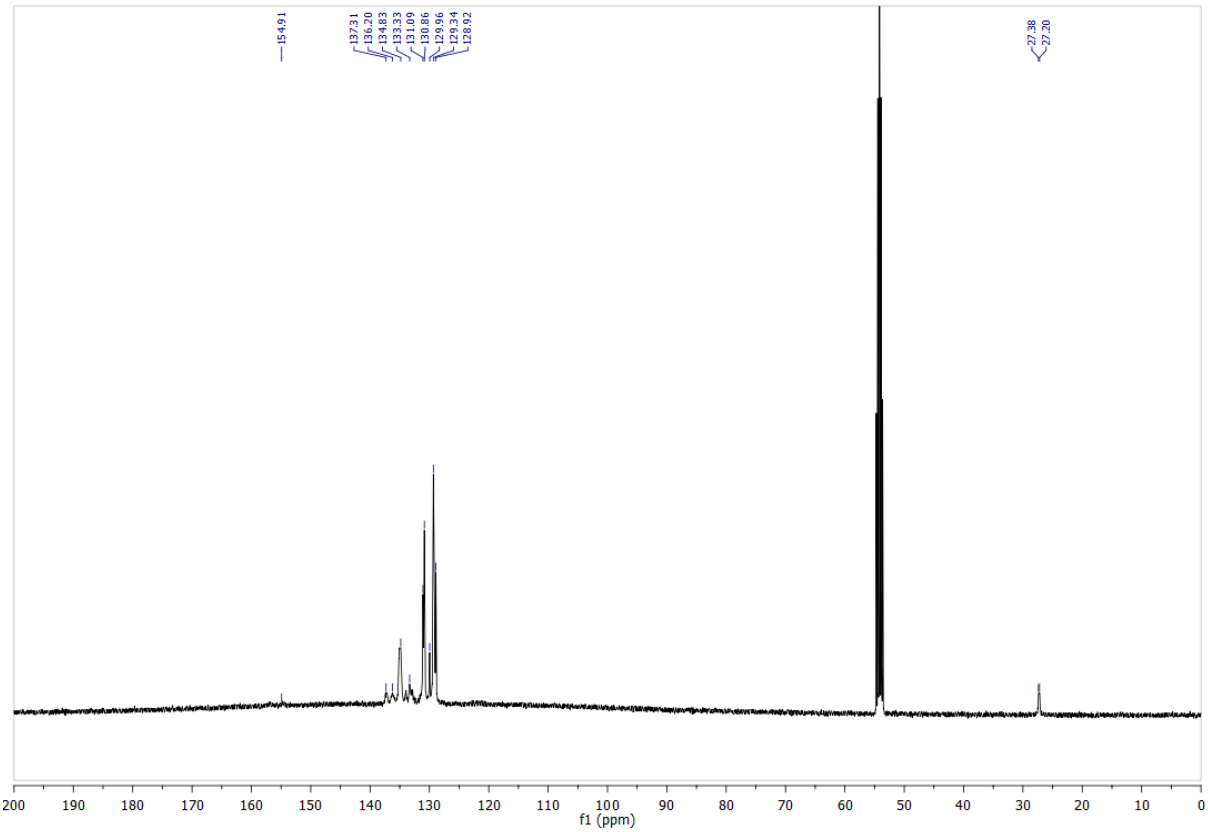

Figure S3. $^{13}C\{^{1}H\}$ NMR RT spectrum of the derivative **D**.

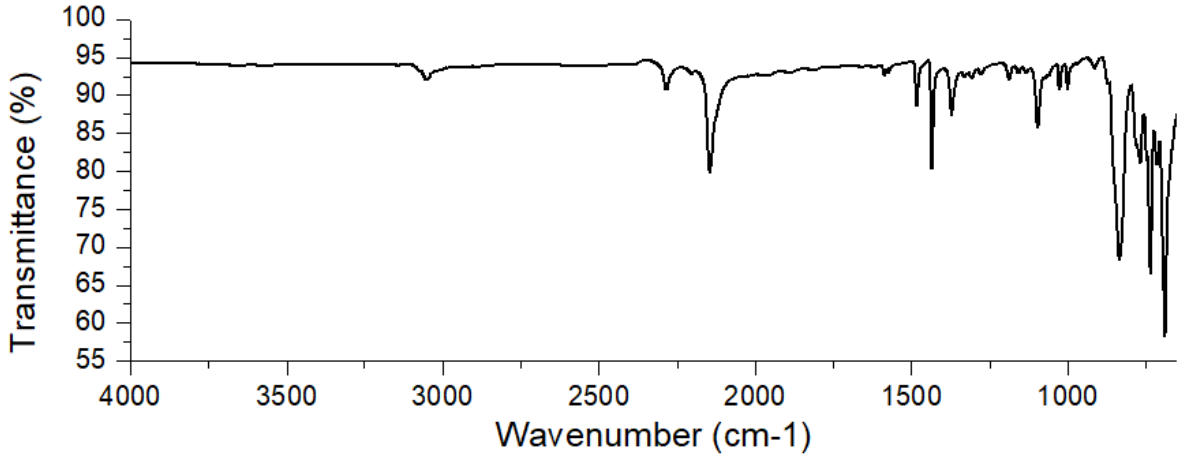

Figure S4. IR spectrum of **D** in the solid state.

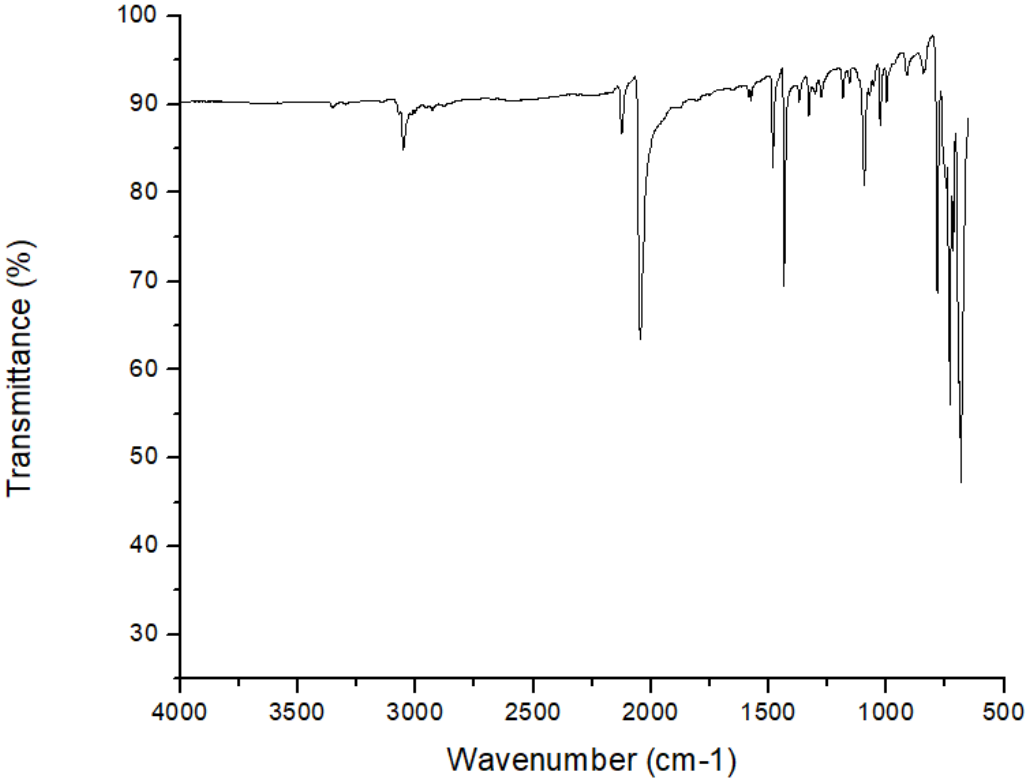

Figure S5. IR spectrum of **E** in the solid state.

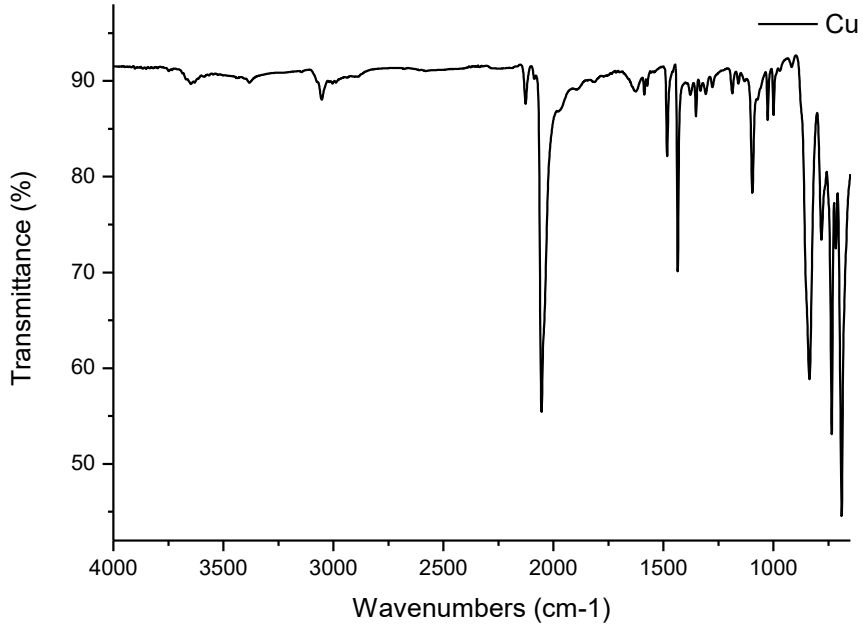

Figure S6. IR spectrum of $\mathbf{F}_{Cu}$ in the solid state.

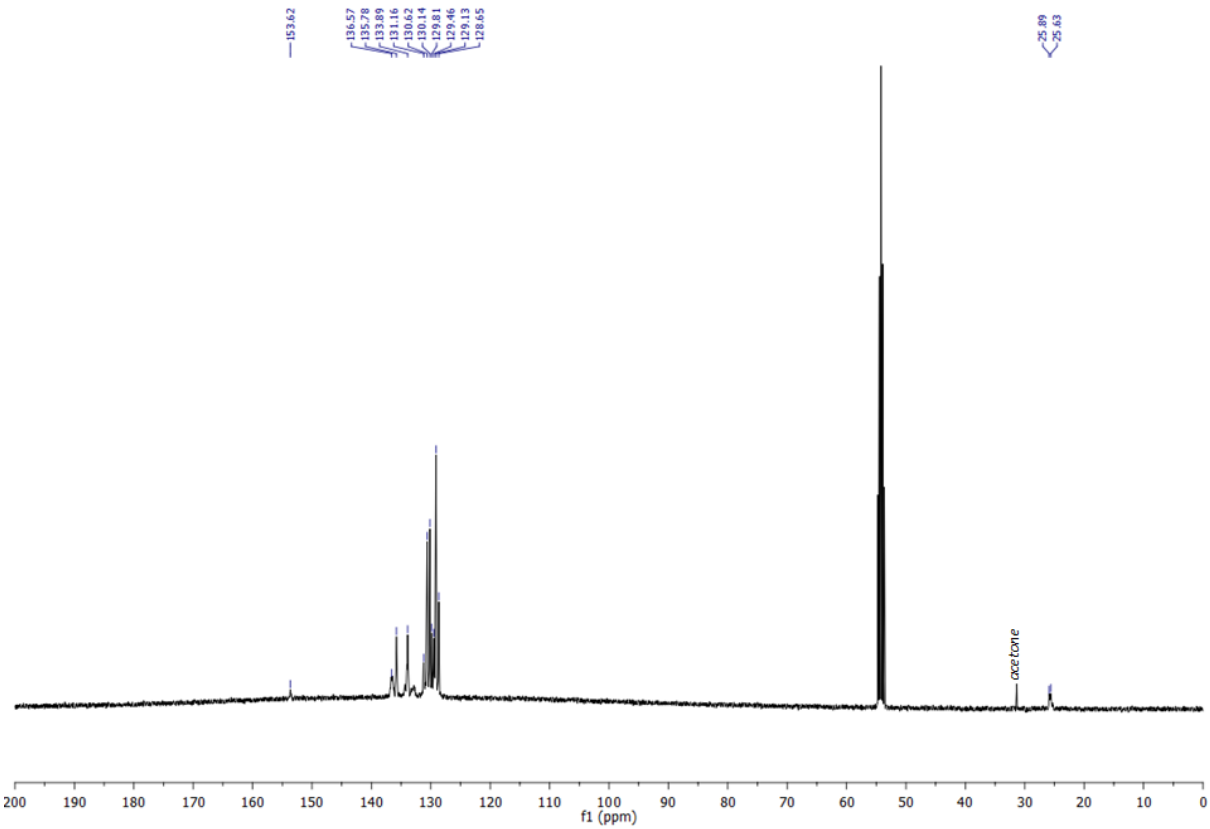

Figure S7. $^{13}C\{^{1}H\}$ NMR RT spectrum of the derivative $\mathbf{F_{Zn}}$.

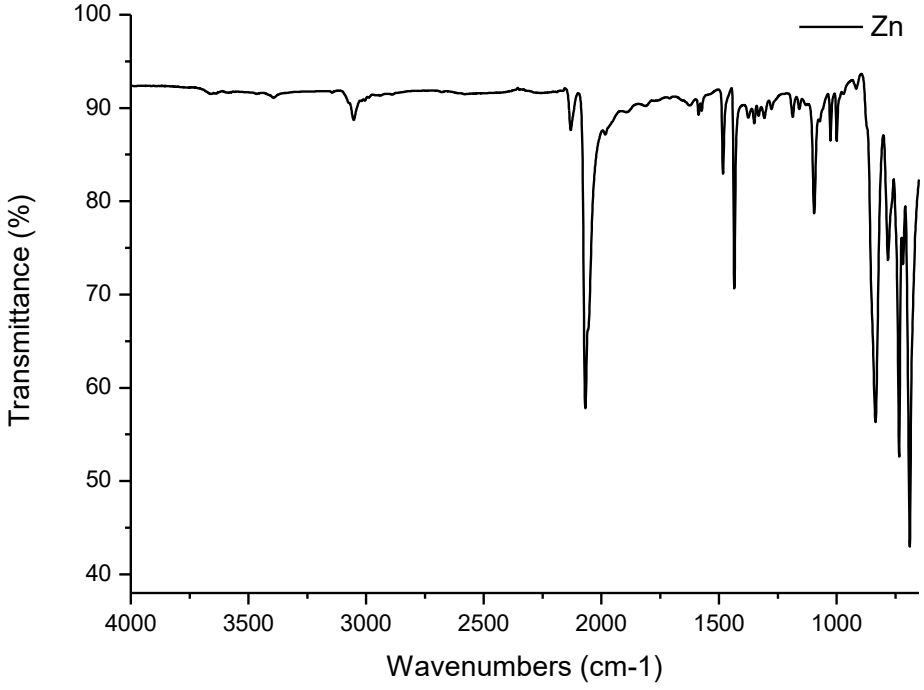

Figure S8. IR spectrum of $\mathbf{F_{Zn}}$ in the solid state.

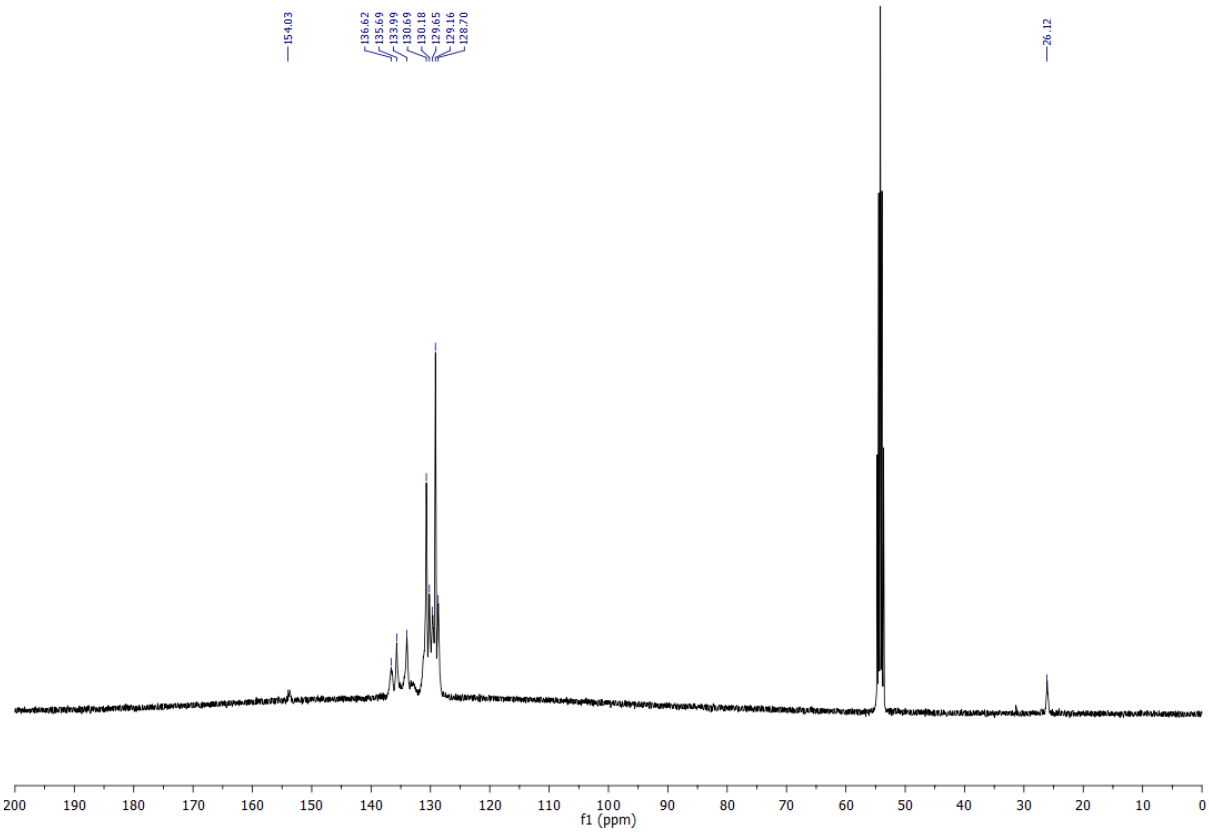

Figure S9. $^{13}C\{^{1}H\}$ NMR RT spectrum of the derivative $\mathbf{F}_{Cd}$.

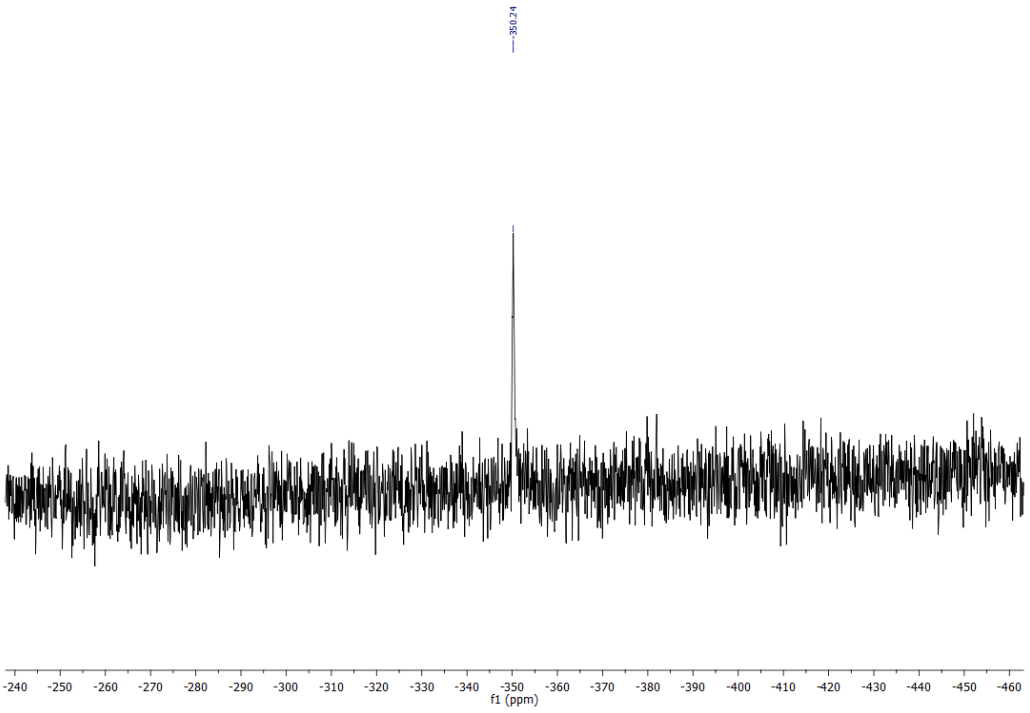

Figure S10. ^{113}Cd NMR RT spectrum of the derivative $\mathbf{F}_{Cd}$.

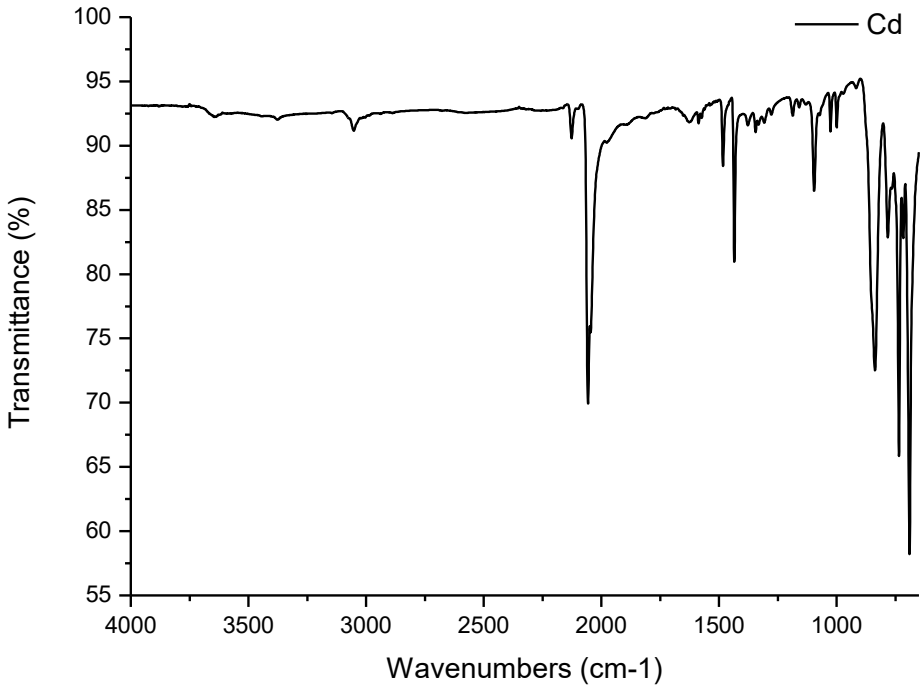

Figure S11. IR spectrum of $\mathbf{F}_{Cd}$ in the solid state.

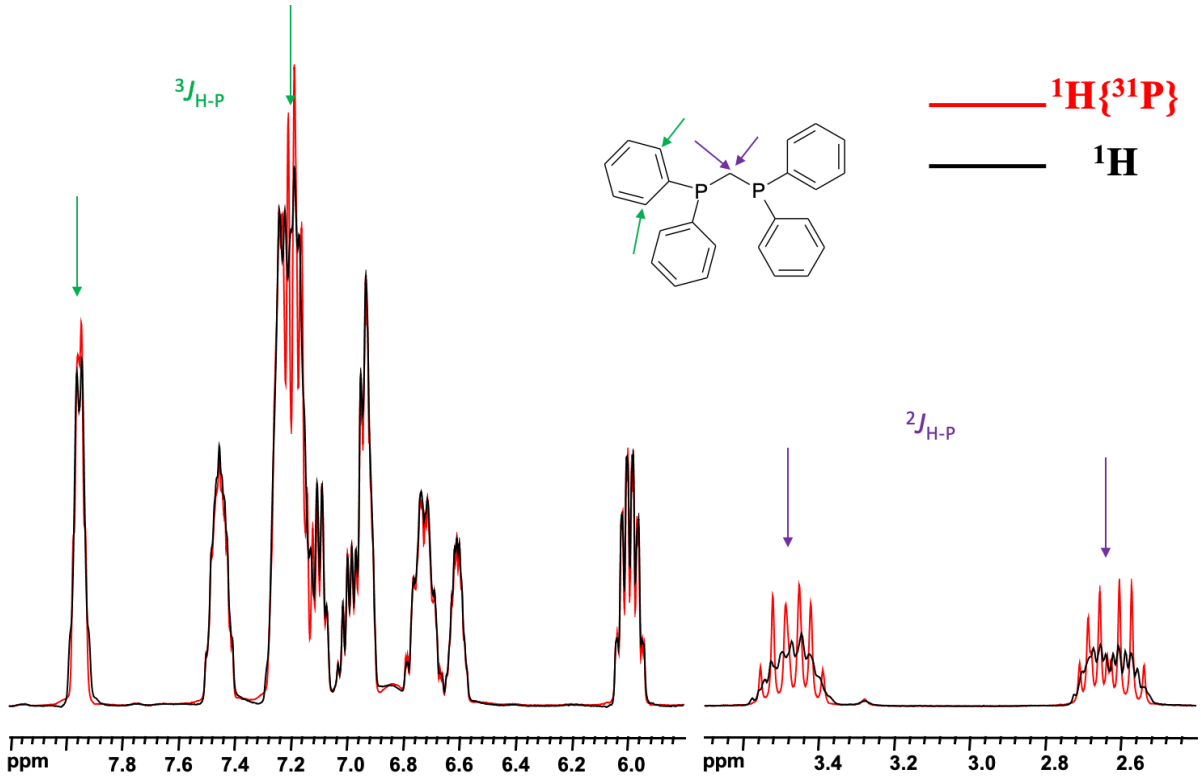

Figure S12. Comparison between ^1H (black line) and $^1H\{^{31}P\}$ (red line) NMR RT spectra of $\mathbf{F}_{Zn}$, highlighting the effects of J_{H-P} coupling.

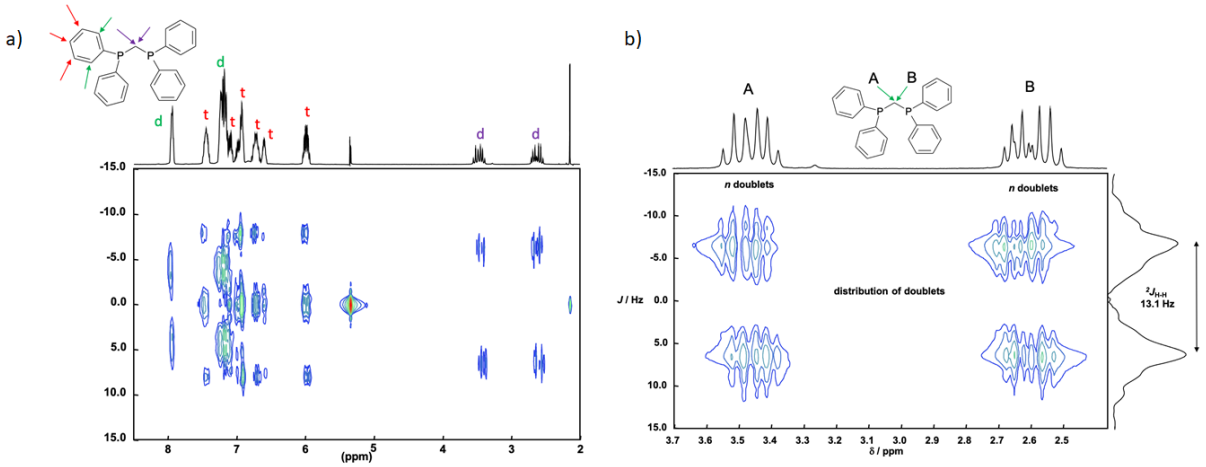

Figure S13: a) $^{1}H\{^{31}P\}$ *J*-Resolved 2D NMR RT spectrum of $\mathbf{F_{Zn}}$, evidencing the $J_{H\text{-}H}$ coupling. Thus, the spectrum is composed of triplets and doublets (overlapped) patterns in the aromatic range and overlapping doublets for the methylenic protons (2.5 – 3.5 ppm range); b)**.** $^{1}H\{^{31}P\}$ *J*-Resolved 2D NMR RT spectrum of $\mathbf{F_{Zn}}$ in the methylenic protons range (2.3 – 3.7 ppm), showing that the observed multiplets (A & B) are sets of overlapping doublets. All doublets have nearly the same $J_{H\text{-}H} \approx 13.1$ Hz.

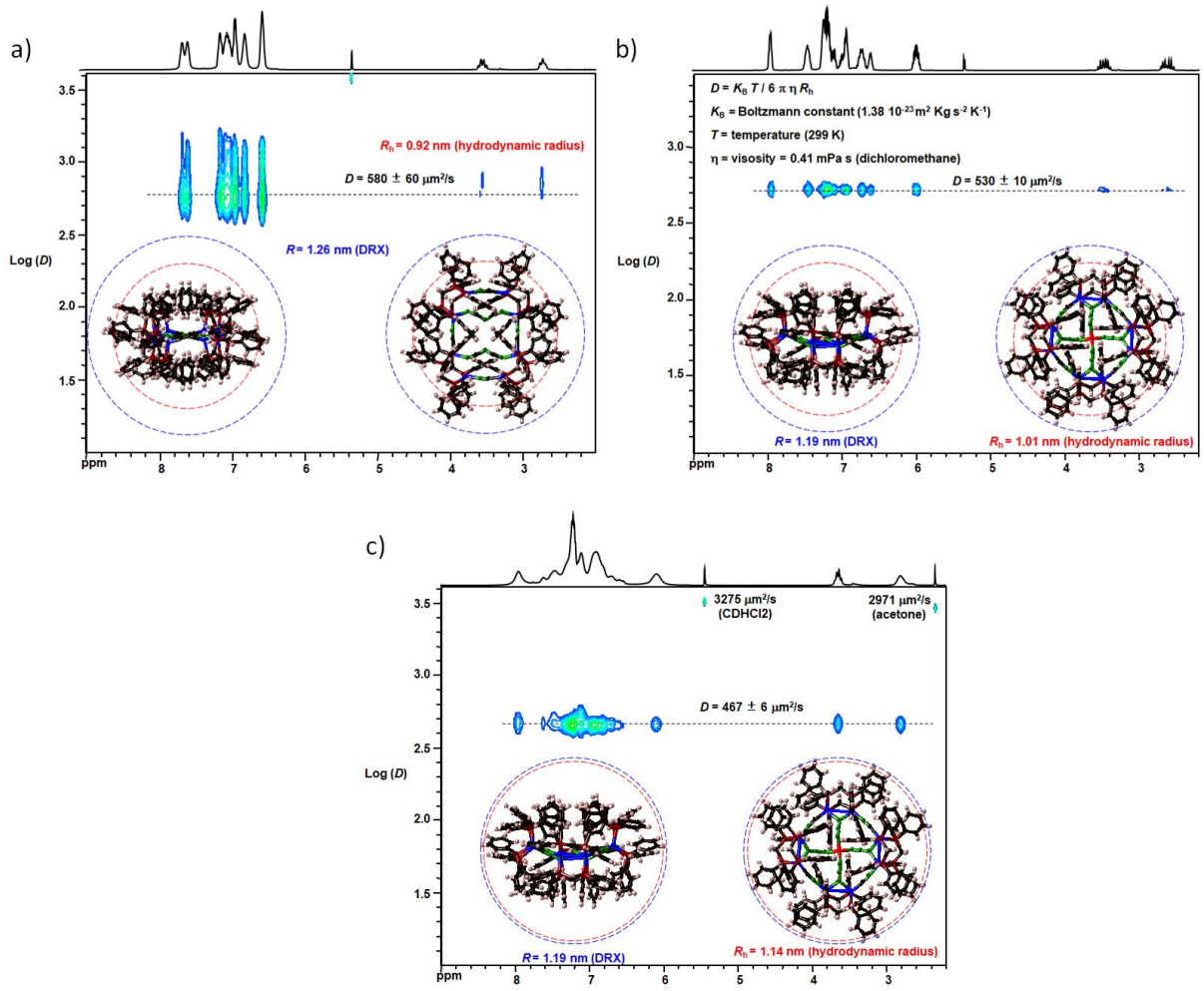

Figure S14: DOSY spectrum of the derivatives : a) **D**; b) $\mathbf{F_{Zn}}$ and c) $\mathbf{F_{Cd}}$.

Table S1 summarizes the observed DOSY diffusion coefficients and the calculated hydrodynamic diameters (2 x R_h) of the precursor **A**, the discrete CDSs **D,** $\mathbf{F_{Zn}}$, $\mathbf{F_{Cd}}$. Globally, the calculated size from the experimental diffusion rates *D*, are quite consistent with XRD dimensions of the molecular species studied (note that the global scaffold of the derivative **D** is significantly more anisotropic and more flexible than $\mathbf{F_{Zn}}$ and $\mathbf{F_{Cd}}$ which may, at less partially cause the larger signals observed). For the polymeric compound **E** the calculated average DOSY sizes (see figure S15) correspond to a molecular building block with two bimetallic units approximatively, respectively. These results indicate that although poorly soluble this polymer dissociated and can be dissolved as small fragments of various nuclearity.

Table S1. Observed diffusion coefficients and calculated hydrodynamic diameters of dissolved **A**, **D, F_{Zn}, F_{Cd}** and **E** in CD_2Cl_2, compared to structural features from XRD data.

	D ($\mu m^2/s$)	2 x R_h (nm)	Number of **A'** units	XRD dimension (nm x nm x nm)	Average dimensions (nm)
E	600 ± 100	1.8 ± 0.3	2	2.3 x 1.4 x 1.3	1.7 ± 0.5
A	590 ± 30	1.8 ± 0.1	2	2.0 x 1.8 x 1.3	1.7 ± 0.3
D	580 ± 60	1.8 ± 0.2	4	2.5 x 2.2 x 1.4	2.1 ± 0.6
F_{Zn}	530 ± 10	2.0 ± 0.1	4	2.4 x 2.4 x 1.4	2.1 ± 0.6
F_{Cd}	467 ± 6	2.3 ± 0.1	4	2.4 x 2.4 x 1.4	2.1 ± 0.6

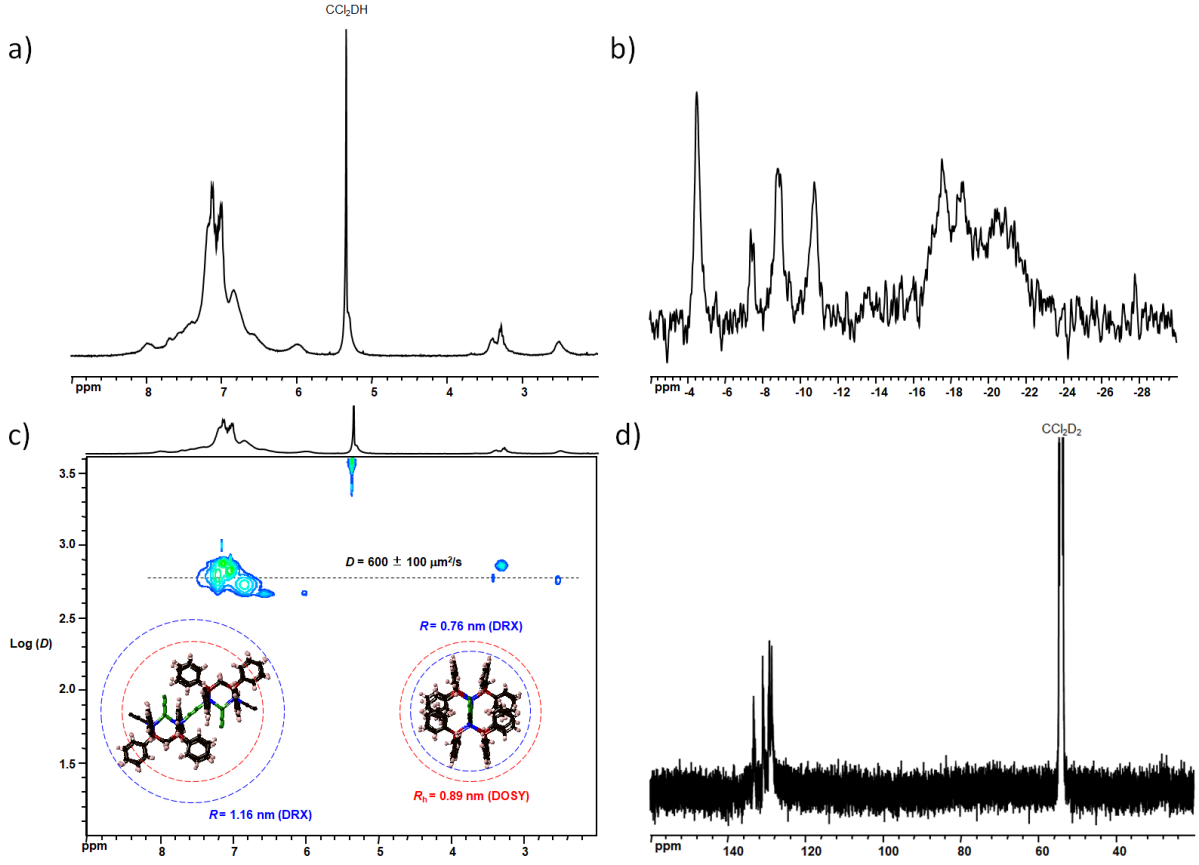

Figure S15: NMR spectra recorded in CD_2Cl_2 resulting in the dissolution and the oligomerization of the 1D-CP derivative **E** a) ^{1}H NMR spectrum of **E,** b) $^{31}P\{^{1}H\}$ NMR spectrum of **E**, c) DOSY NMR analysis of **E**, d) $^{13}C\{^{1}H\}$ NMR spectrum of **E**.

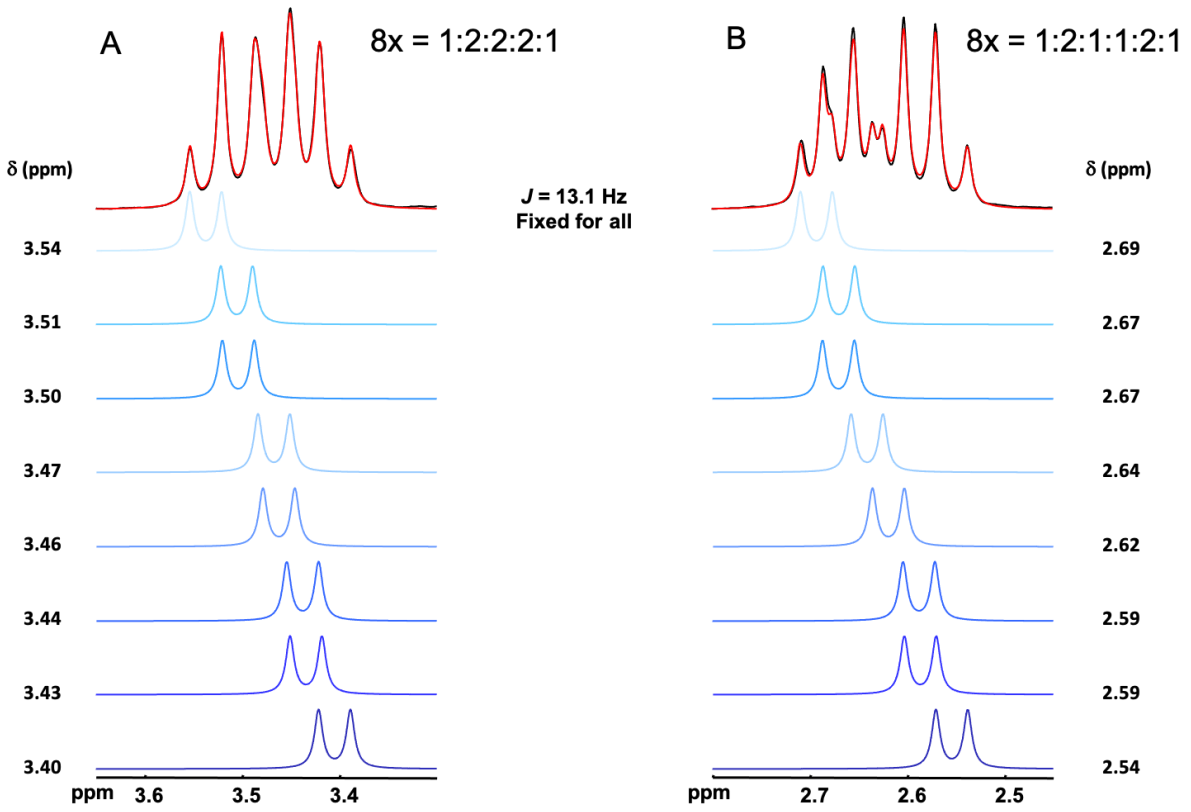

Figure S16. Spectral decomposition of $^{1}H\{^{31}P\}$ NMR resonances for methylenic protons in $\mathbf{F}_{Zn}$, using 8 equal doublets with $J_{H\text{-}H} \approx 13.1$ Hz. Black line = experimental spectrum, Red line = calculated spectrum, Blue lines = components. Chemical shifts of each individual component are indicated. Such decomposition provides unambiguously the preservation of the structural feature of the cation $\{Cu_8(Zn)(N_3)_4(CN)_4dppm_8\}^{2+}$ with 8 independent dppm ligands.

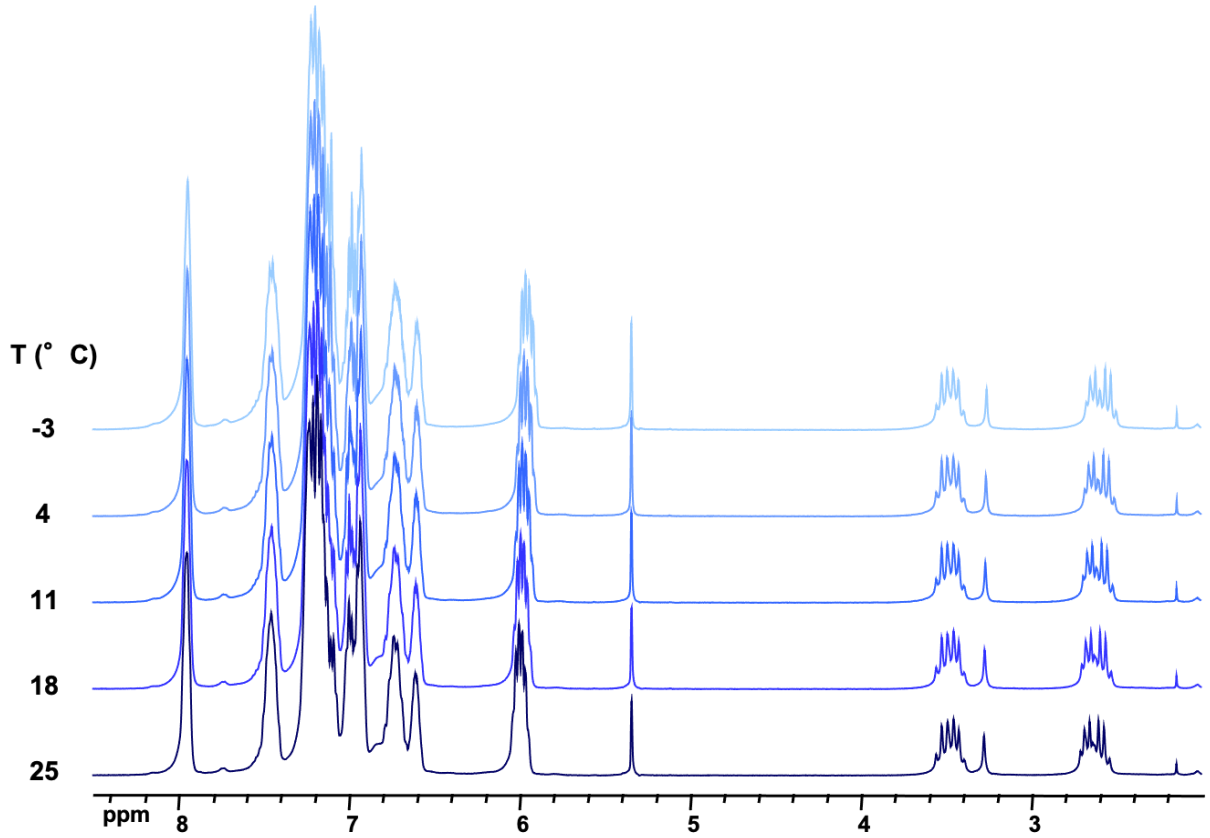

Figure S17. Variable temperature $^{1}H\{^{31}P\}$ NMR spectra of $\mathbf{F}_{Zn}$, showing almost no change within the temperature range 25 to -3 °C.

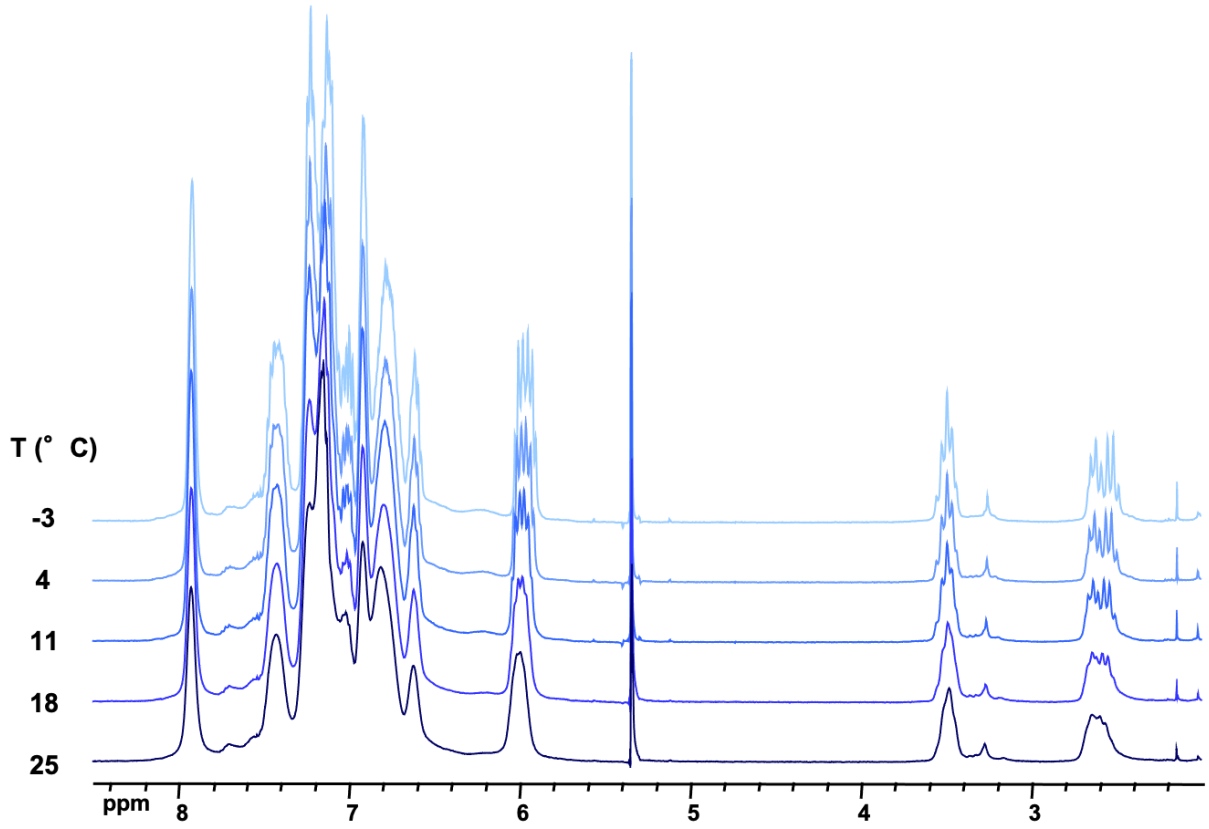

Figure S18. Variable temperature $^{1}H\{^{31}P\}$ NMR spectra of $\mathbf{F}_{Cd}$, featuring the narrowing effect on signals upon lowering the temperature. This results clearly indicate the line broadening observed at RT is due to molecular dynamic effects.

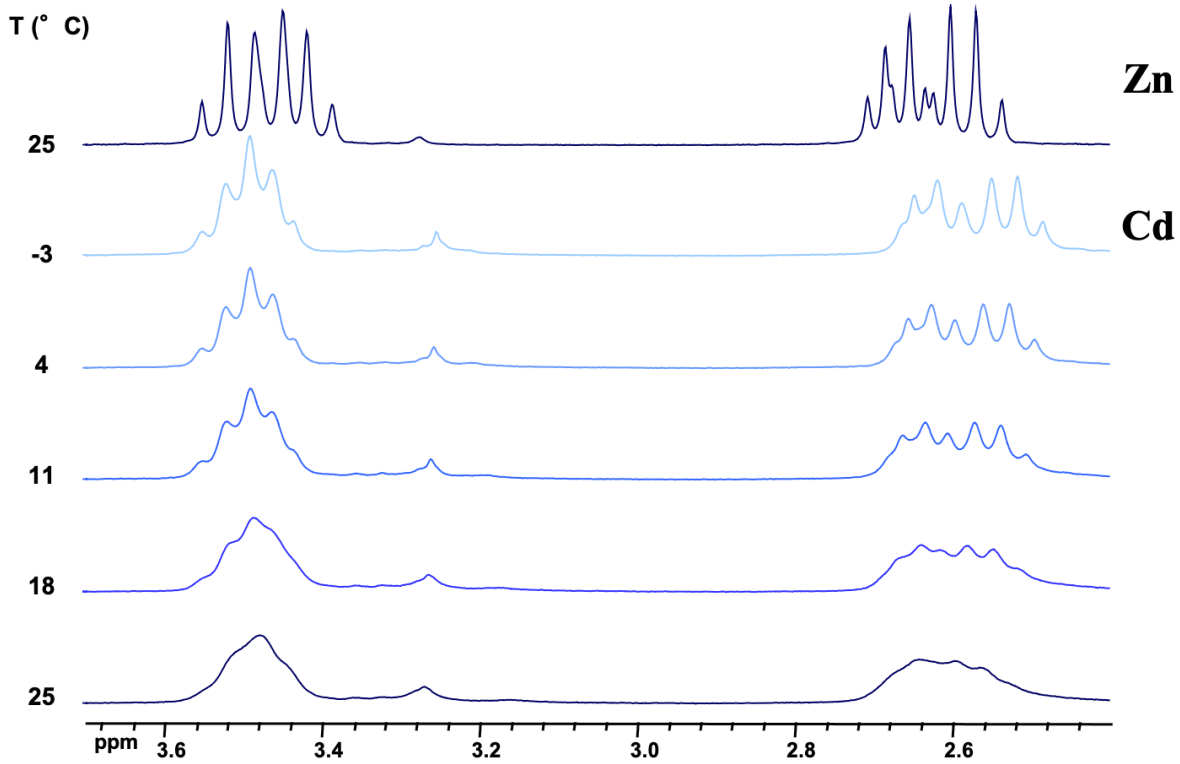

Figure S19. Variable temperature $^{1}H\{^{31}P\}$ NMR spectra of $\mathbf{F}_{Cd}$ in the methylenic protons range (2.3 – 3.7 ppm) compared to the RT spectrum of $\mathbf{F}_{Zn}$.

II. X-ray Crystallographic Study

Single crystal data collection for **D**, **E**, $\mathbf{F}_{Cu}$, $\mathbf{F}_{Zn}$, and $\mathbf{F}_{Cd}$**.** were performed at 150 K with a D8 Venture Bruker AXS (Centre de Diffractométrie, Université de Rennes 1, France) with Mo-*K*α radiation (λ = 0.71073 Å). Reflections were indexed, Lorentz-polarization corrected and integrated by the *DENZO* program of the KappaCCD software package. The data merging process was performed using the SCALEPACK program.[S5] Structure determinations were performed by direct methods with the solving program SIR97, [S6] that revealed all the non-hydrogen atoms. SHELXL program[S7] was used to refine the structures by full-matrix least-squares based on F^2. All non-hydrogen atoms were refined with anisotropic displacement parameters.

Single crystals of all these derivatives were always coated in paratone oil, mounted at low temperature on the diffractometer goniometer as quickly as possible in the case of the solvated crystals **D** and **E**. The single crystals of derivatives $\mathbf{F}_{Cu}$, $\mathbf{F}_{Zn}$, and $\mathbf{F}_{Cd}$ were treated the same way concerning the fact that these crystals kept their single-crystal integrity once removed from the mother solution and dried. X-ray data collection were performed at low temperature. In all cases, in the crystal lattices of the coordination complexes studied, dichloromethane solvent molecules were found in addition to the cationic coordination complexes and their counter-anions.

The included dichloromethane solvent molecules were found to be highly disordered and a correct modelling of the disorder of these solvent molecules was not always possible leading to rather high anisotropic displacement parameters for some of their atoms. We have therefore proceeded to a 'squeeze' treatment[S8] in order to remove the scattering contribution of these molecules which cannot be satisfactorily modelled (5.5 CH_2Cl_2 molecules per asymmetric unit for derivative **D**, 2 CH_2Cl_2 molecules per asymmetric unit for derivative **E,** 0.5 CH_2Cl_2 molecules per asymmetric unit for derivatives $\mathbf{F}_{Cu}$, $\mathbf{F}_{Zn}$, and $\mathbf{F}_{Cd}$). In the case of the derivatives $\mathbf{F}_{Cu}$, $\mathbf{F}_{Zn}$, and $\mathbf{F}_{Cd}$ hexafluorophosphate counter-anions were also found very disordered and the a 'squeeze' treatment[S8] also removed the scattering contribution of these molecules which cannot be satisfactorily modelled. As a result, since these disordered molecules occupy a significant volume of the unit cell, several ALERTs A appear in the checkcif reports since " VERY LARGE Solvent Accessible VOIDs" are present in the structure resolution.

Concerning the derivative **D**, the central nitrogen atoms of the two DCM ligands (namely N(201) and N(451)) are found with high anisotropy parameters inducing thermal ellipsoids excessively extended in a direction perpendicular to the mean plane of the octametallic metallacycle sub-unit of **D**. This is very likely the result of a statistic delocalisation of these atoms (and the coordinated DCM ligands) inside the metallacyccle sub-unit of **D.** Yet, a modelling of this delocalisation was not possible, leading to unstable refinement cycles. Therefore, these DCM ligands were modelled in an average orientation which induces at the level of the N(201) and N(451)

atoms these high anisotropy parameters that are associated with an ALERT A and an ALERT B in the checkcif report of **D**. In addition, equal relative occupancies for the C and N atoms have been modelled at the atomic position determined for the all the cyano ligands, atoms which have been refined with isotropic displacement parameters.

Concerning the derivative **E**, single crystals of **E** were always obtained as extremely tiny needles. Despite several attempts performed on single crystal batches from different preparations, diffraction pattern were extremely weak. Yet, unit cell determination measurements always revealed the same parameters, giving confidence in the homogeneity of the bulk polycrystalline batches afforded by these syntheses. In one case only, one single crystal presented a diffraction pattern of sufficient intensity and quality to allow a measurement to be performed. Yet, it was not possible to collect a data set to allow to proceed to a X-ray crystal structure resolution of sufficient quality. Therefore, only a structural model for the gross molecular structure of **E** can be supplied from this measurement, but the metric data cannot be analysed in detail. It results of this for the derivative **E** that final agreement (R) factors were determinate with modest values (Table S1) and several ALERTs level B appear in the checkcif reports. Only heavy atoms (phosphorus and copper) where treated with anisotropic displacement parameters and the other atoms of this 1D-CP were refined with isotropic displacement parameters. Yet, gross structural parameters observed in the structural model established for **E** are in full agreement with those determined for related compounds (including derivatives **D**, $\mathbf{F}_{Cu}$, $\mathbf{F}_{Zn}$, and $\mathbf{F}_{Cd}$) for which X-ray crystal structure determination could be satisfactory performed. This gives strong confidence about the pertinence of the structural model determined for the 1D-CP **E**

Concerning the derivatives, $\mathbf{F}_{Cu}$, $\mathbf{F}_{Zn}$, and $\mathbf{F}_{Cd}$, one phenyl ring of the dppm ligands in the assymetric unit was found disordered over two neighboring positions and the relative occupancies were ponderated. Yet, despite this modelling, refinement cycles converged toward high anisotropy parameters for some of the atoms modelled inducing several ALERT A and an ALERT B in the checkcif reports. In addition, equal relative occupancies for the C and N atoms have been modelled at the atomic position determined for the all the cyano ligands, atoms which have been refined with isotropic displacement parameters.

Table S2 gives the crystallographic data for the derivatives **D**, **E**, $\mathbf{F}_{Cu}$, $\mathbf{F}_{Zn}$, and $\mathbf{F}_{Cd}$.

Atomic scattering factors for all atoms were taken from International Tables for X-ray Crystallography.[S9] CCDC reference numbers 2081510, 2081507, 2081509, 2081504 and 2081508 contain the supplementary

crystallographic data for the reference measurements of the X-ray crystal structures of the derivatives **D**, **E**, $\mathbf{F}_{Cu}$, $\mathbf{F}_{Zn}$, and $\mathbf{F}_{Cd}$ respectively. These data can be obtained free of charge from the Cambridge Crystallographic Data Centre.

Table S2. Crystal data and structure refinement for derivatives **D**, **E**, $\mathbf{F}_{Cu}$, $\mathbf{F}_{Zn}$, and $\mathbf{F}_{Cd}$, after the 'squeeze' treatment (values in italic are related to the relevant data before the squeeze treatment).

	D	**E**[a]	$\mathbf{F}_{Cu}$	$\mathbf{F}_{Zn}$	$\mathbf{F}_{Cd}$
Molecular formula	$C_{208}H_{176}Cu_8F_{12}N_{10}P_{18}$ *($C_{219}H_{184}Cu_8F_{12}N_{10}P_{18}Cl_{23}$)*	$C_{51}H_{44}Cu_2N_4P_4$ *($C_{53}H_{46}Cu_2N_4P_4Cl_4$)*	$C_{204}H_{176}Cu_9N_{16}P_{16}$ *($C_{208}H_{184}Cu_9N_{16}P_{18}Cl_8F_{12}$)*	$C_{204}H_{176}Cu_8N_{16}P_{16}Zn$ *($C_{208}H_{184}Cu_8N_{16}P_{18}ZnCl_8F_{12}$)*	$C_{204}H_{176}CdCu_8N_{16}P_{16}$ *($C_{208}H_{184}Cu_8N_{16}P_{18}CdCl_8F_{12}$)*
CCDC number	2081510	2081507	2081509	2081504	2081508
Molecular weight	4109.36 *(5117.35)*	963.86 *(1131.70)*	3918.98 *(4540.57)*	3920.81 *(4542.40)*	3967.84 *(4589.43)*
a(Å)	26.213(2)	12.838(2)	40.354(4)	40.219(4)	40.445 (3)
b (Å)	24.552(2)	14.184(2)	40.354	40.219	40.445
c (Å)	35.205(3)	14.771(2)	40.354	40.219	40.445
α (°)	90	74.249(5)	90	90	90
β (°)	102.646(3)	81.760(5)	90	90	90
γ (°)	90	72.726(5)	90	90	90
V (Å^3)	22108(3)	2466.2(6)	65714 (6)	65057(6)	66160 (5)
Z	4	2	12	12	12
*D*c (g cm^{-3})	1.235 *(1.526)*	1.298 *(1.524)*	1.188 *(1.377)*	1.201 *(1.391)*	1.195 *(1.382)*
Crystal system	Monoclinic	Triclinic	Cubic	Cubic	Cubic
Space group	C 2/c	P-1	I -4 3d	I -4 3d	I -4 3d
Temperature (K)	150(2)	150(2)	150(2)	150(2)	150(2)
Wavelength Mo-*K*α (Å)	0.71069	0.71069	0.71073	0.71073	0.71073
Crystal size (mm)	0.25 * 0.15 * 0.10	0.08 * 0.02 * 0.01	0.16 * 0.14 * 0.11	0.14 * 0.11 * 0.08	0.12 * 0.10 * 0.09
μ (mm^{-1})	0.943 *(1.228)*	1.029 *(1.251)*	1.022 *(1.148)*	1.045 *(1.172)*	1.015 *(1.140)*
F(000)	8416 *(10304)*	992 *(1156)*	24156 *(27732)*	24168 *(27744)*	24384 *(27960)*
θ limit (°)	2.18 – 27.49	2.56 – 27.61	2.26 – 27.47	2.265 –27.495	2.25 – 27.49
Index ranges *hkl*	-26 ≤*h*≤ 34, -31 ≤*k*≤ 31, -45 ≤*l*≤ 45	-16 ≤*h*≤ 16, -18 ≤*k*≤ 18, -15 ≤*l*≤ 19	-46 ≤*h*≤ 52, -52 ≤*k*≤ 52, -51 ≤*l*≤ 52	-52 ≤*h*≤ 52, -52 ≤*k*≤ 50, -52 ≤*l*≤ 52	-52 ≤*h*≤ 52, -50 ≤*k*≤ 52, -52 ≤*l*≤ 52
Reflections collected	86041	45998	296831	359799	288903
Independant reflections	25271	10994	12555	12469	12679
Reflections [$I>2\sigma(I)$]	18680 *(18811)*	5483	11159 *(9614)*	11435 *(10235)*	11679 *(10570)*
Data/restraints/ parameters	25271/ 0 / 1440 *(1305)*	10994/ 0 / 263 *(308)*	12555/ 0 / 582 *(662)*	12469/ 0 / 582 *(662)*	12679/ 0 / 582 *(662)*
Goodness-of-fit on F^2	1.068 *(1.038)*	1.102 *(1.209)*	1.153 *(1.133)*	1.100 *(1.124)*	1.100 *(1.144)*
Final *R* indices [$I>2\sigma(I)$]	R1= 0.0472 *(0.0685)* wR2= 0.1143 *(0.1713)*	R1= 0.1915 *(0.2101)* wR2= 0.4194 *(0.4438)*	R1= 0.0706 *(0.0754)* wR2= 0.1476 *(0.1862)*	R1= 0.0521*(0.0586)* wR2= 0.1294 *(0.1476)*	R1= 0.0574 *(0.0727)* wR2= 0.1406 *(0.1901)*
R indices (all data)	R1= 0.0660*(0.0975)* wR2= 0.1208 *(0.1929)*	R1= 0.2614 *(0.3045)* wR2= 0.4501 *(0.4845)*	R1= 0.0803 *(0.1104)* wR2= 0.1522 *(0.2205)*	R1= 0.0575 *(0.0831)* wR2= 0.1328 *(0.1775)*	R1= 0.0625 *(0.0956)* wR2= 0.1446 *(0.2237)*
Largest diff peak and hole (e Å^{-3})	1.059 and -1.146 *(3.626 and -1.539)*	4.050 and -1.834 *(3.358 and -2.226)*	0.463 and -0.400 *(1.417 and -0.725)*	0.500 and -0.408 *(0.726 and -0.571)*	0.648 and -0.407 *(1.385 and -0.897)*

[a]: Only a structural model for the gross molecular structure of **E** can be supplied from this measurement, but the metric data can not be analysed in details

Table S3. Selected intermetallic distances [Å] and angles [°] in the derivatives **D**, **E**, $\mathbf{F}_{Cu}$, $\mathbf{F}_{Zn}$, and $\mathbf{F}_{Cd}$ **(**Only a structural model for the gross molecular structure of **E** can be supplied from this measurement, but the metric data can not be analysed in details)

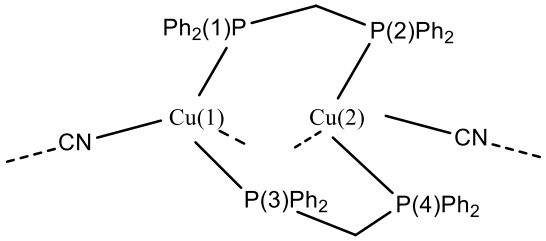

	D	**E**	$\mathbf{F}_{Cu}$	$\mathbf{F}_{Zn}$	$\mathbf{F}_{Cd}$
Cu(1)-Cu(2)	3.4173(8) 3.4346(8)	3.23	3.354(1)	3.313(1)	3.357(1)
Cu(1)-'CN'	1.975(9) 2.041(14)	1.98	2.07(9)	1.99(3)	1.9829(7)
Cu(2)-'CN'	1.996(11) 2.027(11)	1.95	2.06(5)	2.03(3)	1.9638(8)
Cu(1)-P(1)	2.2617(8) 2.2689(9)	2.23	2.251(2)	2.2511(16)	2.251(2)
Cu(1)-P(3)	2.2672(9) 2.2512(8)	2.25	2.256(2)	2.2523(15)	2.2528(18)
Cu(2)-P(2)	2.2325(8) 2.2738(9)	2.25	2.249(2)	2.2473(16)	2.2490(18)
Cu(2)-P(4)	2.2556(9) 2.2545(8)	2.23	2.257(2)	2.2559(16)	2.2530(19)
Cu-N_{DCM}	2.069(2) 2.101(2)	-	-	-	-
Cu-N_{N3}	-	2.09 2.09	2.149(6) 2.134(6)	2.172(5) 2.165(4)	2.158(5) 2.136(6)
M^{II}-N_{N3}	-	-	1.943(6)	1.997(4)	2.177(6)
N_{N3}-M^{II}-N_{N3}	-	-	132.1(4) 99.48(14)	121.8(3) 103.69(12)	121.9(3) 103.64(14)

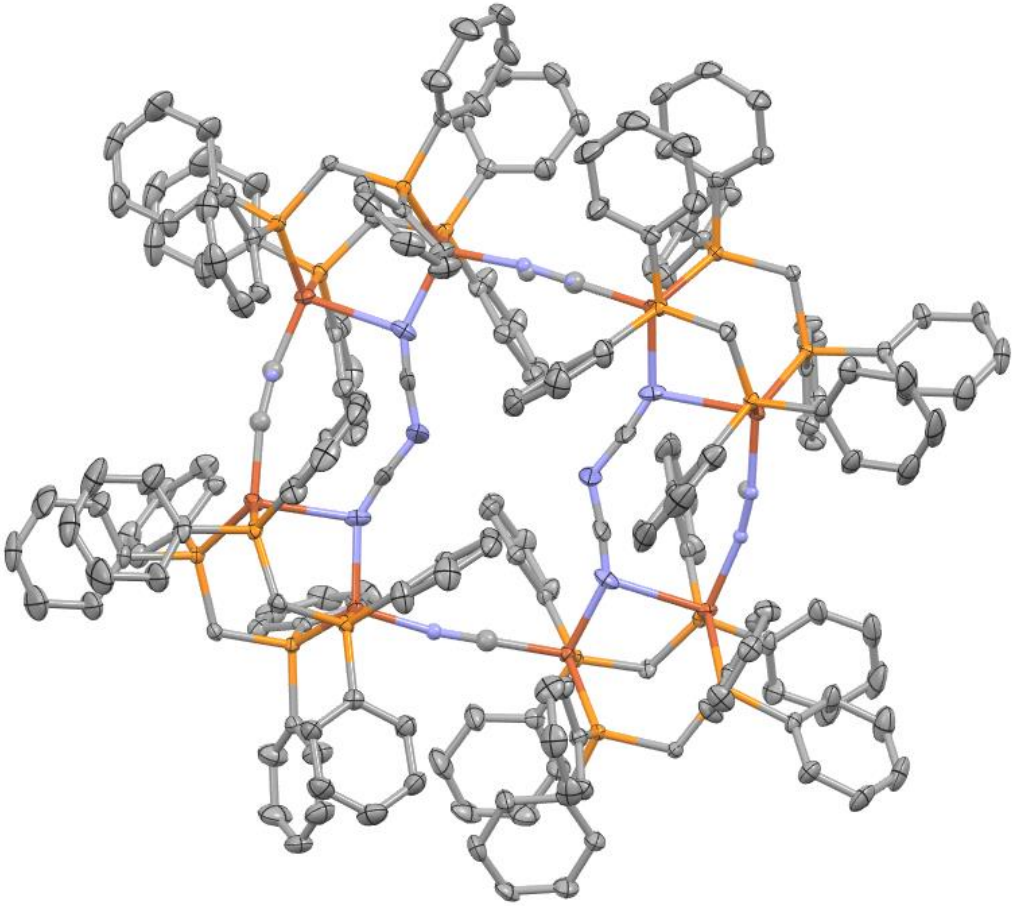

Figure S20. ORTEP views of the molecular structure of the dicationic derivative **D**. Hydrogen atoms, hexafluorophosphate counter-anions and included CH_2Cl_2 solvent molecules have been omitted for clarity. Atoms color codes: dark orange: copper, light orange : phosphorus, grey : carbon, blue : nitrogen.

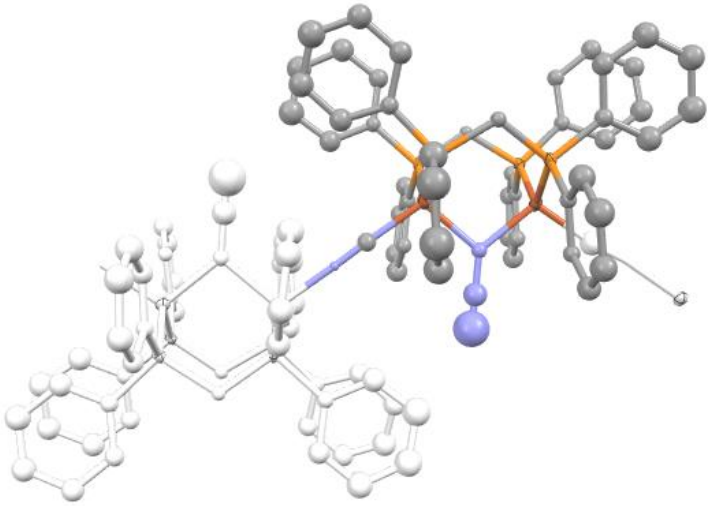

Figure S21. ORTEP views (only the copper and phosphorus atoms have been modelled with anisotropic displacement parameters) of a fragment of the molecular structure of the neutral 1D-CP **E**. Hydrogen atoms and included CH_2Cl_2 solvent molecules have been omitted for clarity. One repetition unit is shown in color while the connected fragments are shown in white. Atoms color codes for the repetition unit in colors: dark orange: copper; light orange: phosphorus; grey: carbon, blue: nitrogen. Only a structural model for the gross molecular structure of **E** can be supplied from this measurement, but the metric data cannot be analysed in details.

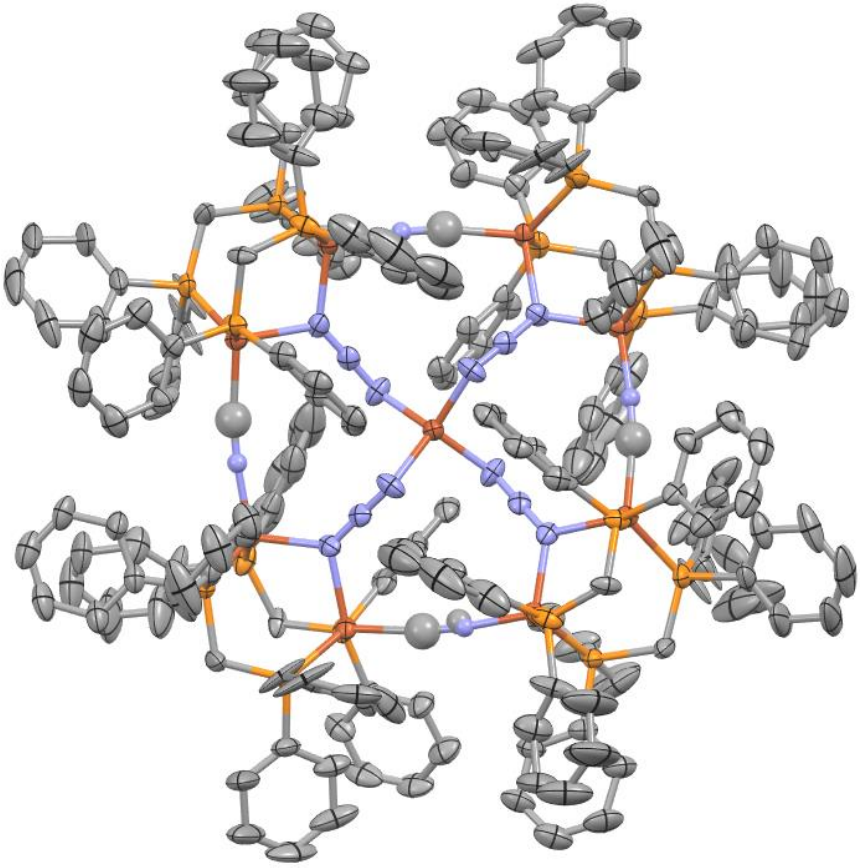

Figure S22. ORTEP views of the molecular structure of the dicationic derivative $\mathbf{F}_{\boldsymbol{Cu}}$. Hydrogen atoms, hexafluorophosphate counter-anions and included CH_2Cl_2 solvent molecules have been omitted for clarity. Atoms color codes for the repetition unit in colors: dark orange: copper; light orange: phosphorus; grey: carbon, blue: nitrogen.

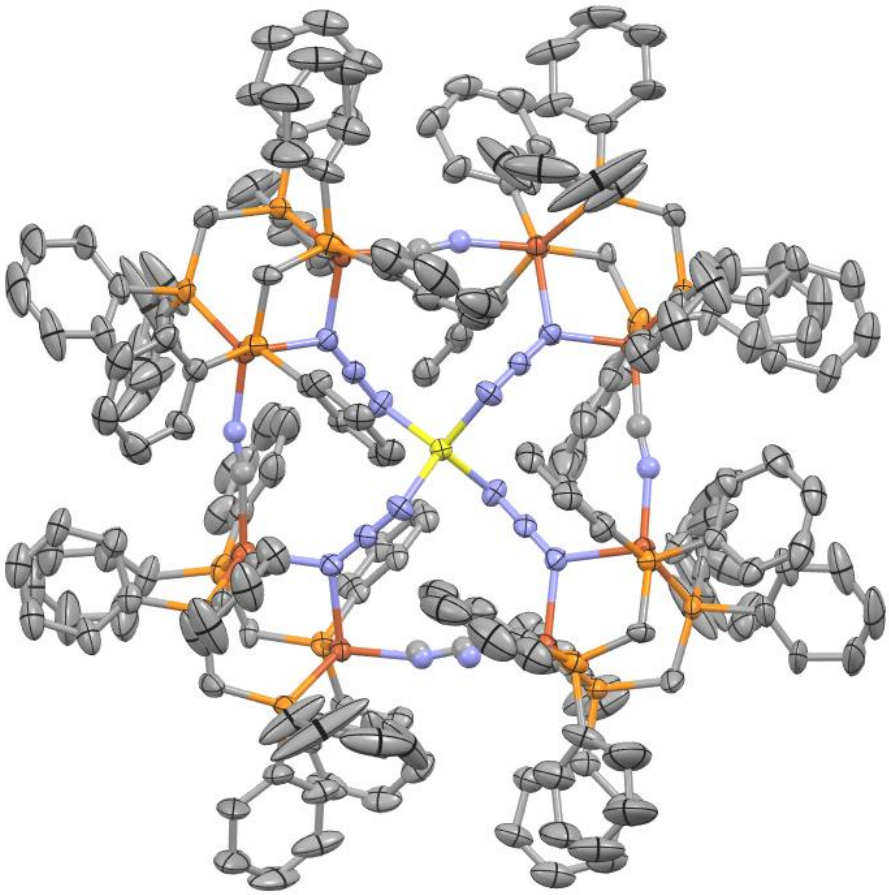

Figure S23. ORTEP views of the molecular structure of the dicationic derivative $\mathbf{F_{Zn}}$. Hydrogen atoms, hexafluorophosphate counter-anions and included CH_2Cl_2 solvent molecules have been omitted for clarity. Atoms color codes for the repetition unit in colors: dark yellow: zinc; light orange: phosphorus; grey: carbon, blue: nitrogen.

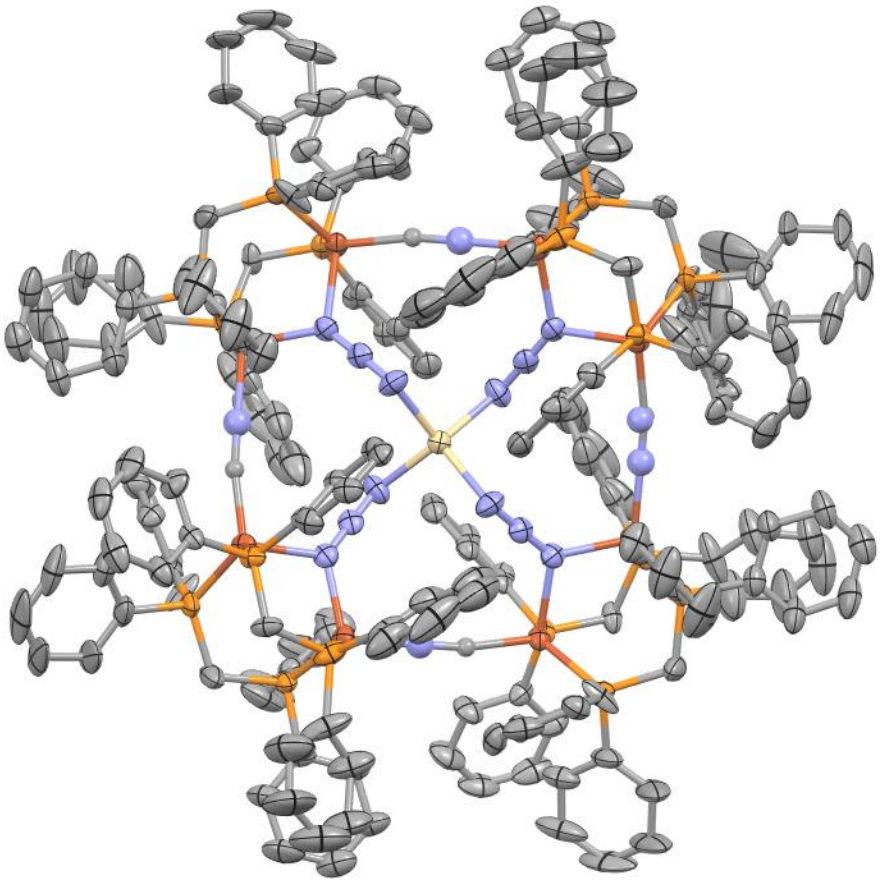

Figure S24. ORTEP views of the molecular structure of the dicationic derivative $\mathbf{F}_{\boldsymbol{Zn}}$. Hydrogen atoms, hexafluorophosphate counter-anions and included CH_2Cl_2 solvent molecules have been omitted for clarity. Atoms color codes: dark yellow: cadmium; light orange: phosphorus; grey: carbon, blue: nitrogen.

III. Photophysical study

The analysis of the photophysical study of the derivative **D** is detailed in the main text of the article. The thermal variation of the emission spectra of the 1D-CP **E** is characterized by a weak and large band centered at ca. 600 nm (λ_{ex} = 394 nm) that does not show noticeable shift upon temperature cooling (Figure S35), featuring a low temperature eye-perceived orange luminescence. Similarly, the temperature-dependence of the emission spectra of $\mathbf{F_{Zn}}$ shows a very weak large band centered at ca. 520 nm (λ_{ex} = 340 nm) that also does not shift with temperature changes (Figure S36), being associated with a low temperature eye-perceived yellowish luminescence. While compounds **E** and $\mathbf{F_{Zn}}$ appear non-luminescent in the solid state at RT, $\mathbf{F_{Cd}}$ presents a weak eye-perceived yellowish luminescence at 290 K associated with a large band centered at 490 nm (λ_{ex} = 330 nm, figure S37) and a RT EQY of 2%. Upon cooling, this band presents a net intensity enhancement together with a slight red-shift resulting at 80 K in a large band centered at 505 nm (λ_{ex} = 330 nm, figure S37).

Table S4. Photophysical data for derivatives **D**, $\mathbf{F_{Cu}}$, $\mathbf{F_{Zn}}$, and $\mathbf{F_{Cd}}$ in the solid state.

	λ_{em} (nm)[a]	Φ_{em}	τ_{obs} (μs)[a]
D (λ_{ex} = 365 nm)	500 (512)	13	52.18 [c] (238.56) [c]
E (λ_{ex} = 394 nm)	600 (605)	- [b]	ca. 7 (32)
$\mathbf{F_{Zn}}$ (λ_{ex} = 330 nm)	520 (520)	- [b]	- [b]
$\mathbf{F_{Cd}}$ (λ_{ex} = 330 nm)	490 (505)	2	- [b]

[a] Data recorded at 80 K are given in parentheses; [b] Not measured due to the very weak intensity of the signal; [c] emissive lifetime of the long-lived component, see Fig. S32

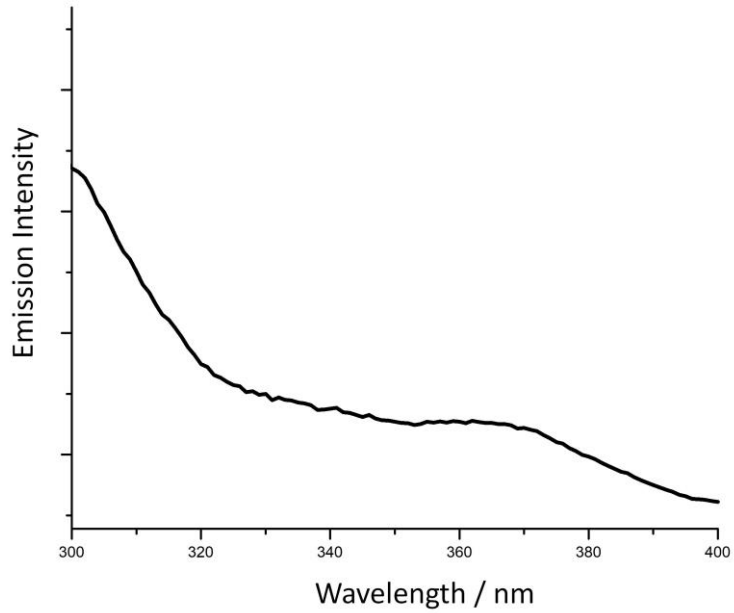

Figure S25. RT solid state excitation spectrum of **D** at 298 K

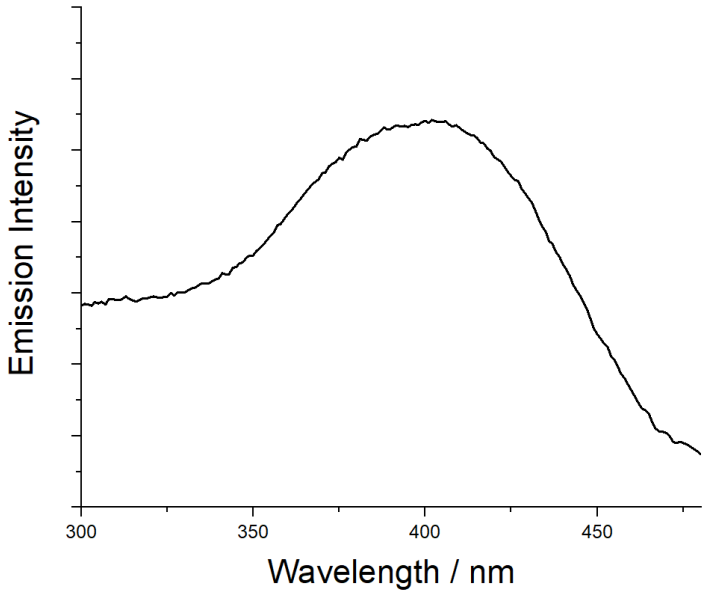

Figure S26. RT solid state excitation spectrum of **E** at 298 K

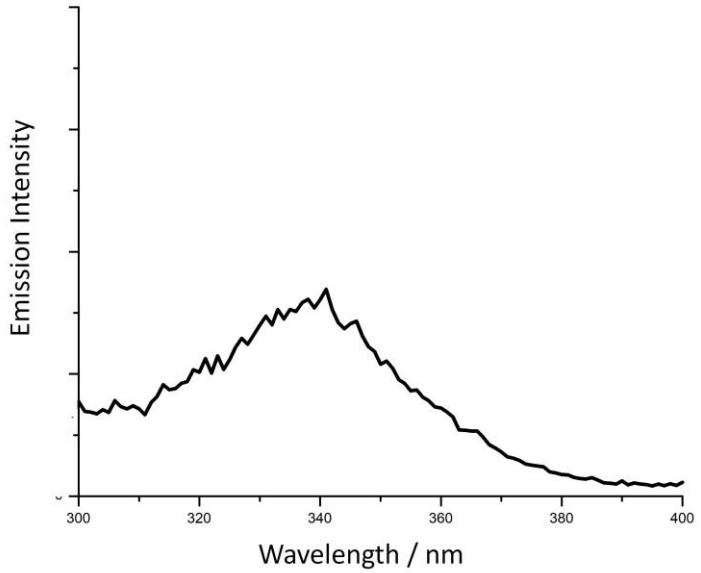

Figure S27. RT solid state excitation spectrum of $\mathbf{F}_{Cd}$ at 298 K

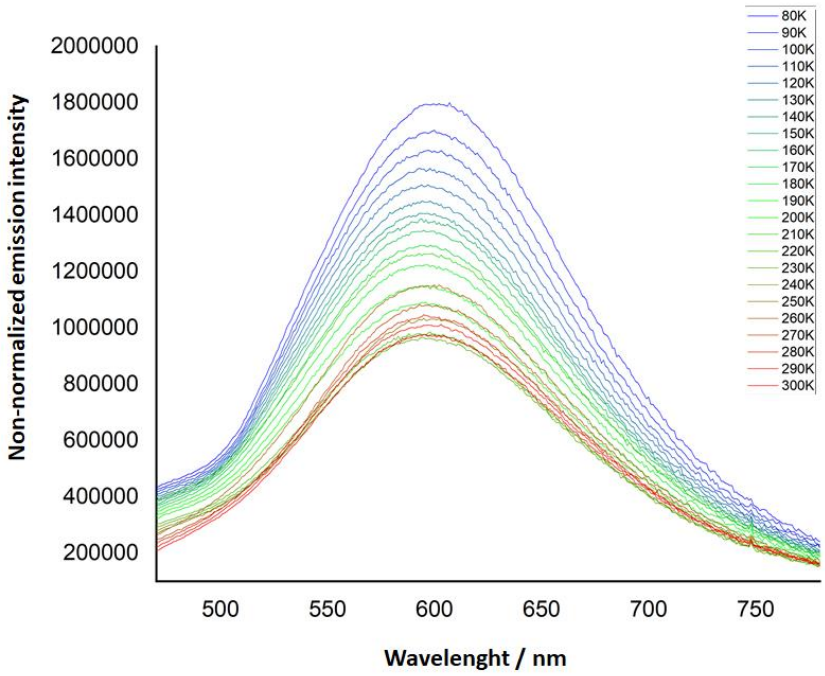

Fig. S28. Temperature-dependent non-normalized (arbitrary units) solid state emission spectra of **E** with λ_{exc} = 394 nm.

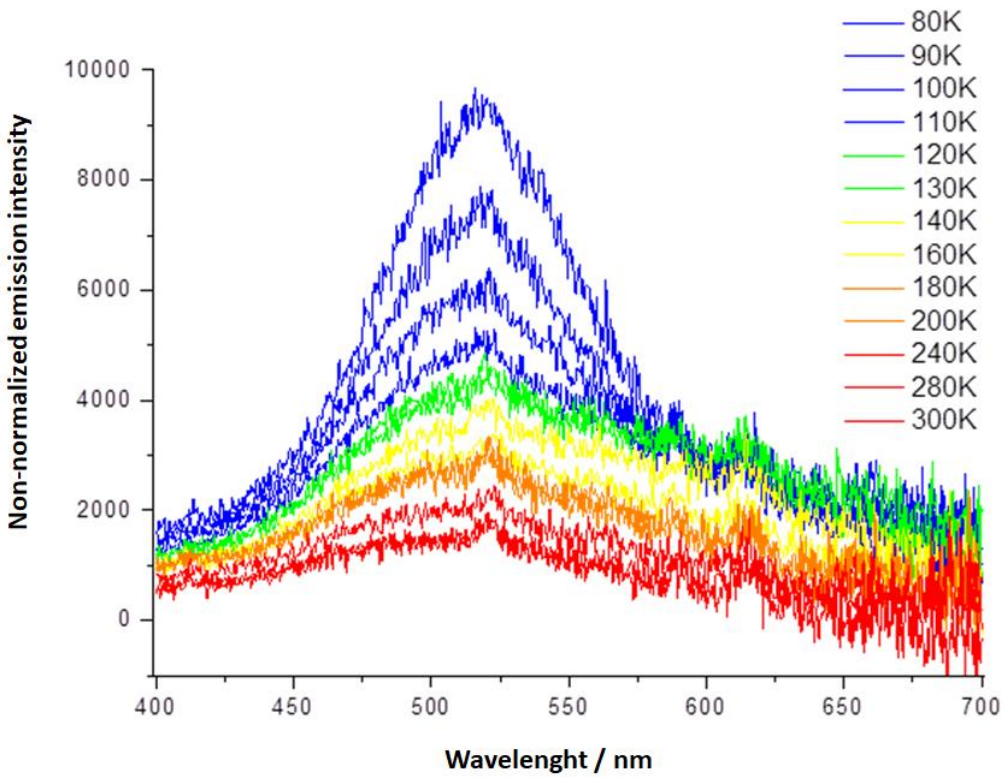

Figure S29. Temperature-dependent non-normalized (arbitrary units) solid state emission spectra of $\mathbf{F}_{\boldsymbol{Zn}}$ with λ_{exc} = 330 nm.

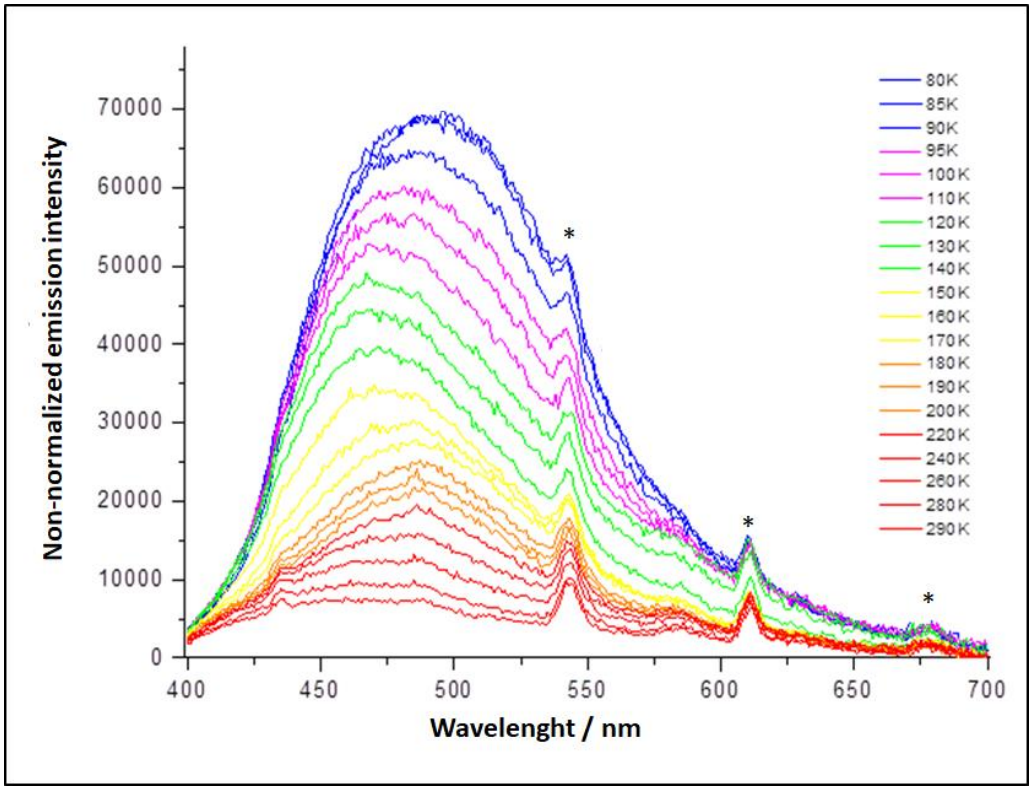

Figure S30. Temperature-dependent non-normalized (arbitrary units) solid state emission spectra of $\mathbf{F}_{Cd}$ with λ_{exc} = 330 nm (the asterisk represents an instrument measurement artefact).

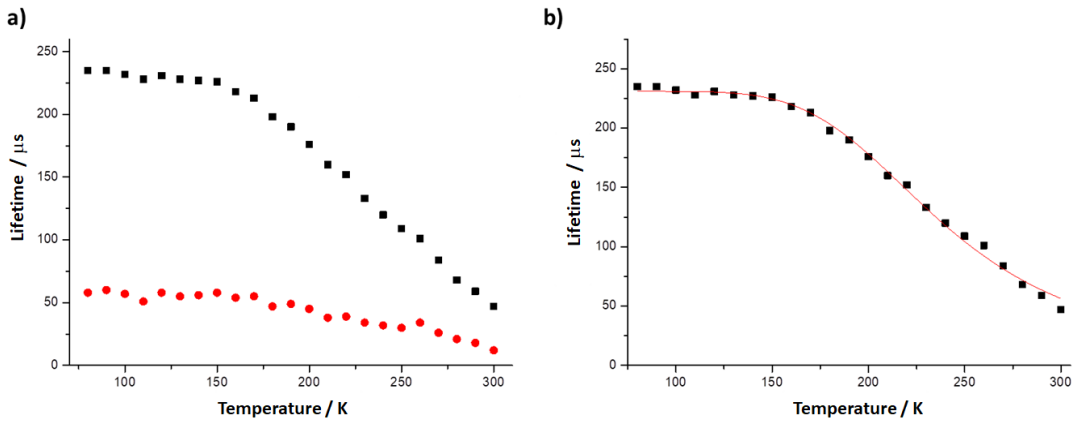

Figure S31. Plot of bi-exponential emission decay lifetime against temperature (80 K to 300 K) of **D** with λ_{exc} = 365 nm: a) thermal variation the two components τ_1 (long-lived component, black dots) and τ_2 (short-lived component, red dots); b) fit of the thermal variation of the τ_1 component to the Boltzmann-type equation S1.

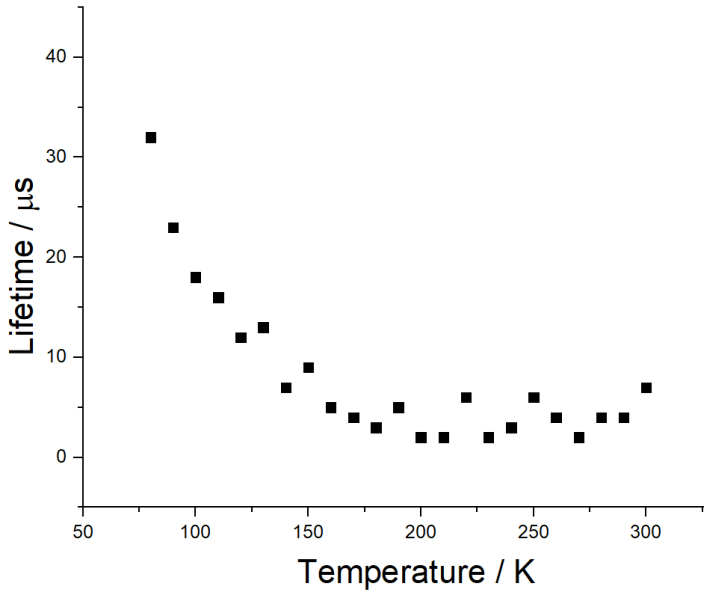

Figure S32. Plot of emission decay lifetime against temperature (80 K to 300 K) of **E** with λ_{exc} = 394 nm (the irregular profile observed is due to the very low intensity of the luminescence signal of **E**).

IV. X-ray powder diffraction diagrams for derivatives F_{Cu}, F_{Zn} and F_{Cd}.

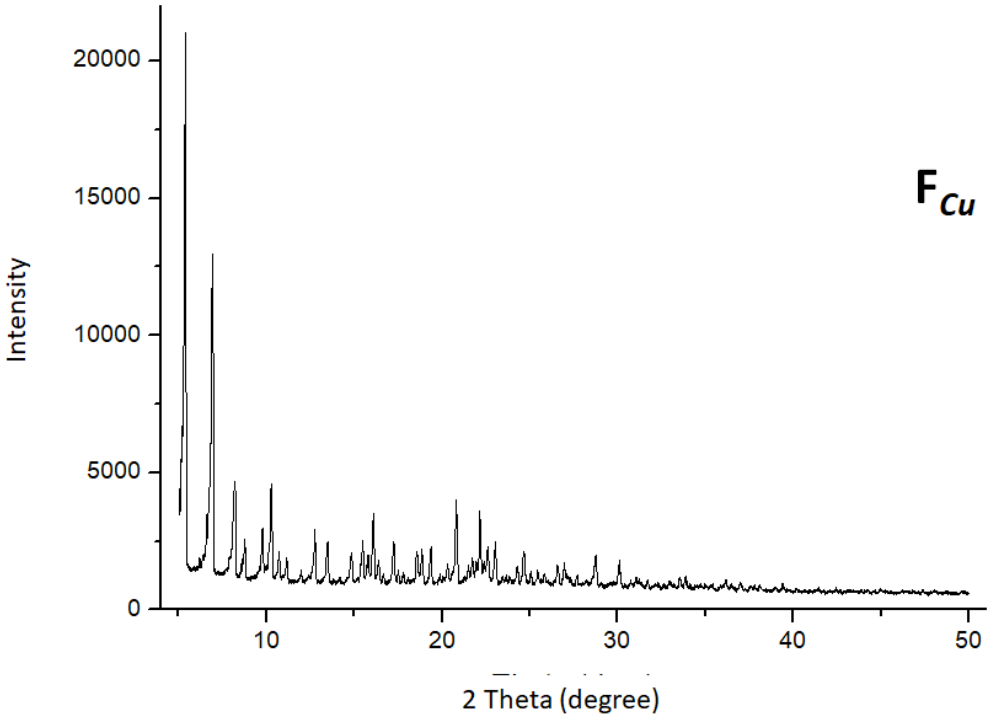

Figure S33: PXRD pattern of F_{Cu} in the solid state.

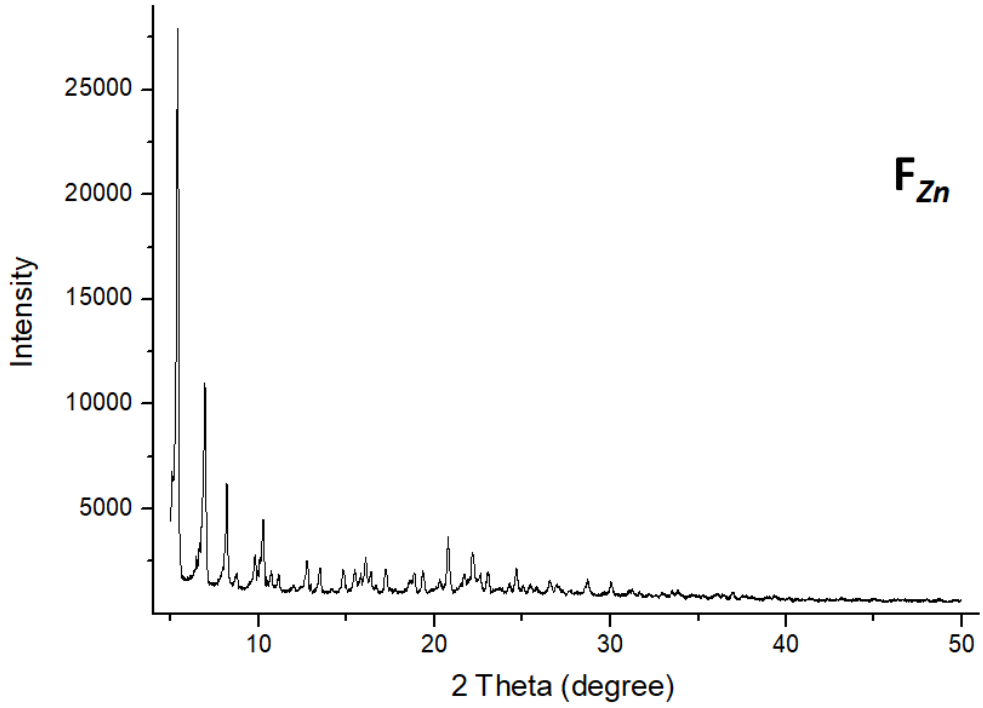

Figure S34: PXRD pattern of $\mathbf{F_{Zn}}$ in the solid state.

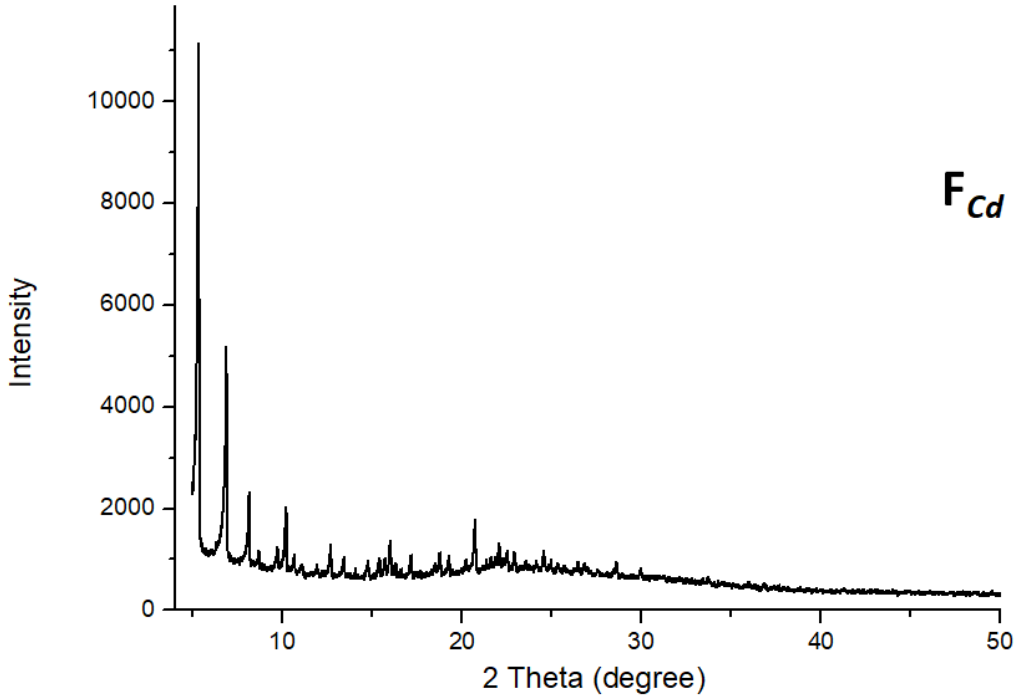

Figure S35: PXRD pattern of $\mathbf{F_{Cd}}$ in the solid state.

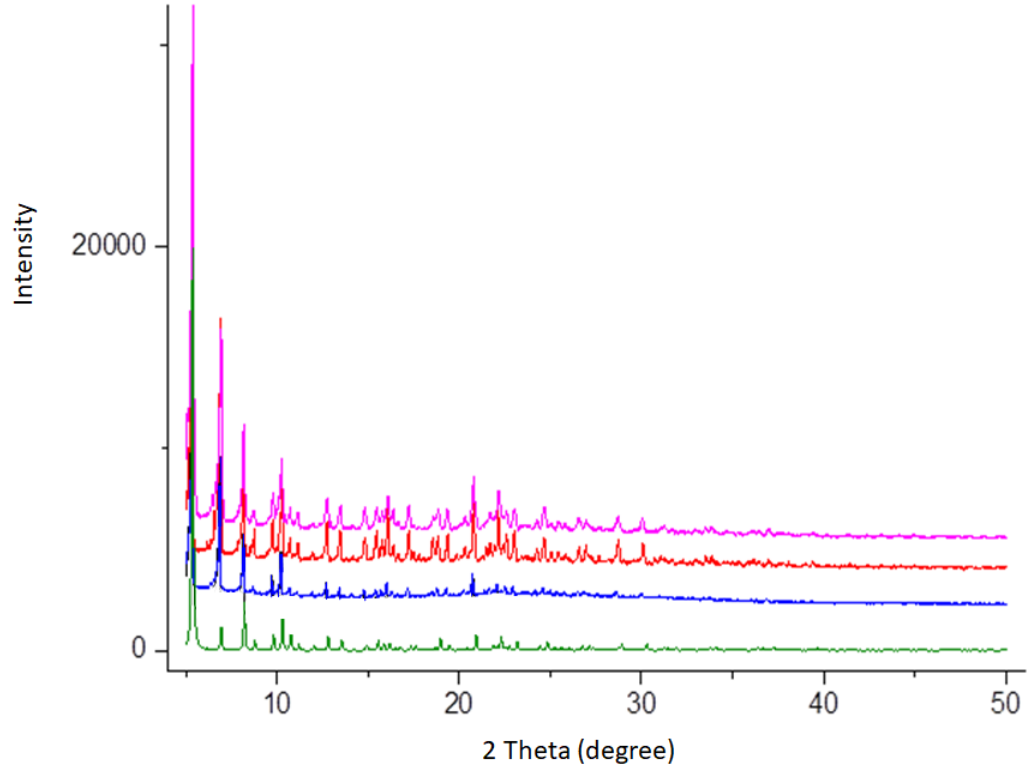

Figure S36: Comparison of the experimental PXRD patterns of $\mathbf{F}_{Cu}$ (red), $\mathbf{F}_{Zn}$ (magenta), $\mathbf{F}_{Cd}$ (blue) in the solid state and the calculated PXRD patterns obtained from the single-crystal X-ray structure of $\mathbf{F}_{Zn}$(Green).

V. Computational details and results

DFT calculations were carried out using the Gaussian 16 program.[S10] The geometries of **D** and $\mathbf{F}_{Cu}$ X-Ray structure (see Scheme S37). All calculations were performed using PBE0[ts11]functional and SVP[s12] atomic basis set. Tight criterion of energy convergence were applied to ensure high quality of calculations (10^{-10} u.a.) since it was not possible to run vibrational frequency calculations which are too demanding in terms of computational resources. The vertical electronic excitation energies of the first vertical singlet and triplet excited states were calculated by time-dependant DFT protocol. Geometry optimizations of the excited states were attempted for both compounds without reaching convergence.

Table S5. Cartesian coordinates of the optimized structures of **D**

D			
Cu	10.525531	12.354665	6.154629
Cu	10.831664	9.467056	4.328400
Cu	11.926752	4.426943	4.385505
Cu	12.165914	1.571645	6.233475
P	12.168310	13.207523	4.742084
P	12.085966	10.700874	2.831420
P	8.368435	12.424929	5.276265
P	8.579411	9.713159	3.767932
P	14.187217	3.945866	3.889546
P	14.431196	1.506569	5.815996
P	10.429997	3.188559	3.084324

P	10.978666	0.504897	4.574729
N	10.918501	9.930855	6.351582
N	10.385836	9.360604	8.679752
N	11.781110	3.887931	6.411586
C	11.902458	15.001309	4.435600
C	12.645267	15.708454	3.479443
H	13.402999	15.198883	2.877839
C	12.446034	17.074531	3.303931
H	13.029346	17.616831	2.555823
C	11.514647	17.753210	4.092228
H	11.364890	18.827180	3.957285
C	10.784760	17.060917	5.054969
H	10.057649	17.585865	5.678274
C	10.975850	15.689297	5.224897
H	10.403588	15.147718	5.982492
C	13.921029	13.244825	5.279264
C	15.005248	12.906383	4.463567
H	14.849824	12.497697	3.464403
C	16.311617	13.082847	4.921310
H	17.148569	12.813680	4.272406
C	16.545884	13.606388	6.190208
H	17.569502	13.753764	6.542627
C	15.469325	13.937992	7.013305
H	15.643578	14.339686	8.014201
C	14.165830	13.748600	6.565384
H	13.325762	14.002831	7.218172
C	12.166352	12.544479	3.016488
H	12.971022	12.976730	2.400439
H	11.212458	12.923576	2.614107
C	13.841308	10.189564	2.650024
C	14.391839	9.334113	3.609093
H	13.765256	8.971143	4.428629
C	15.722427	8.924351	3.504145
H	16.140651	8.247161	4.252365
C	16.507364	9.366256	2.440759
H	17.548022	9.043003	2.358361
C	15.959383	10.209693	1.471320
H	16.568693	10.547040	0.629064
C	14.630066	10.612853	1.570754
H	14.200399	11.252058	0.793783
C	11.489993	10.520159	1.103079
C	11.197062	9.214185	0.682620
H	11.296985	8.382779	1.386936
C	10.772971	8.970446	-0.620214
H	10.540844	7.948416	-0.927422
C	10.622380	10.027018	-1.518808
H	10.282354	9.835805	-2.539369
C	11.334546	11.575378	0.195276
H	11.557010	12.604454	0.486016
C	7.857182	14.129674	4.817451
C	7.528701	15.010414	5.860323
H	7.545367	14.658564	6.895841
C	7.165292	16.325840	5.588606
H	6.898721	16.994007	6.411266
C	7.135485	16.788499	4.272137
H	6.846157	17.819956	4.058006
C	7.475329	15.927253	3.232577
H	7.456768	16.281158	2.199149
C	7.833949	14.605758	3.501955
H	8.087257	13.952097	2.664581
C	6.988049	11.930052	6.382024
C	5.659975	12.270320	6.086170
H	5.430718	12.865244	5.197609
C	4.627832	11.873947	6.931048
H	3.596855	12.149850	6.696379
C	4.911707	11.130311	8.078087
H	4.100623	10.821706	8.742654
C	6.229125	10.791131	8.378509
H	6.460022	10.222277	9.282251
C	7.266839	11.195077	7.537276
H	8.299322	10.943894	7.788544
C	8.006573	11.470709	3.729840
H	8.598192	11.934233	2.922798
H	6.939678	11.564596	3.468726
C	7.398745	8.859442	4.885455
C	7.060543	7.367138	6.762453
H	7.470246	6.735846	7.553204
C	5.680650	7.486813	6.612880
H	5.011483	6.950061	7.290396
C	5.154953	8.282664	5.592441
H	4.073201	8.372676	5.467261
C	7.919283	8.051799	5.901733
H	9.002635	7.954996	6.008264
C	6.010102	8.960967	4.728888
H	5.589519	9.566137	3.921040
C	8.037763	9.072467	2.135319
C	7.404911	9.832796	1.146424
H	7.204089	10.895513	1.297168
C	7.014220	9.239412	-0.055290
H	6.518817	9.844076	-0.818846
C	7.246364	7.884489	-0.278557
H	6.930594	7.422227	-1.216941
C	7.888166	7.121196	0.698280
H	8.086549	6.059583	0.529513
C	8.288772	7.713638	1.891585
H	8.809381	7.114486	2.643026
C	10.900131	11.328270	-1.108046
H	10.784371	12.161114	-1.806022
C	14.934521	3.250500	1.213258
H	14.870336	2.197311	1.495063
C	15.265714	3.569176	-0.104632
H	15.453048	2.767215	-0.822692
C	15.364651	4.900084	-0.501876
H	15.631900	5.146461	-1.532217
C	15.123717	5.915714	0.425080
H	15.201005	6.964837	0.128503
C	14.788827	5.600495	1.738922
H	14.606054	6.408898	2.452319
C	15.394052	4.992527	4.797159
C	16.757329	4.990670	4.468573
H	17.122071	4.374318	3.641797
C	17.653370	5.783575	5.178993
H	18.714670	5.772840	4.918505
C	17.192980	6.594103	6.219365
H	17.894269	7.219865	6.777739
C	15.836984	6.613893	6.539716
H	15.475094	7.261378	7.340958
C	14.938019	5.814382	5.831458
H	13.872215	5.834851	6.071657
C	14.853657	2.236665	4.173537
H	14.338970	1.582375	3.450555
H	15.934105	2.197876	3.957497
C	15.578567	2.273358	7.025014
C	16.965930	2.292812	6.828570
H	17.398440	1.886876	5.909864
C	17.806267	2.802836	7.813315
H	18.887280	2.810911	7.654241
C	17.269590	3.287900	9.008315
H	17.932085	3.672763	9.787985
C	15.891760	3.268489	9.213417
H	15.470032	3.638792	10.151229
C	15.048418	2.761957	8.222742
H	13.969993	2.724749	8.388826
C	15.136000	-0.935019	6.902550

H	14.705916	-0.511692	7.815524
C	15.147640	-0.181844	5.717783
C	15.676336	-2.216607	6.930477
H	15.669989	-2.784834	7.863969
C	16.224825	-2.771868	5.773033
H	16.652630	-3.776999	5.794876
C	16.223211	-2.038596	4.589647
H	16.645840	-2.467628	3.678015
C	15.688749	-0.749380	4.560109
H	15.707676	-0.195180	3.619680
C	10.457549	3.670349	1.306328
C	11.375187	4.642349	0.895781
H	12.036759	5.101503	1.633633
C	11.447859	5.025369	-0.444475
H	12.181567	5.775106	-0.749710
C	10.596012	4.447431	-1.382860
H	10.653270	4.743553	-2.433344
C	9.666142	3.486675	-0.978903
H	8.991583	3.034973	-1.710459
C	9.595647	3.101448	0.357276
H	8.850728	2.360853	0.659792
C	8.639264	3.314998	3.460040
C	8.193367	4.540174	3.973547
H	8.923949	5.311681	4.234573
C	6.831147	4.783033	4.144962
H	6.499140	5.751899	4.523970
C	5.901756	3.790681	3.836085
H	4.833385	3.980103	3.967400
C	6.338025	2.554874	3.360748
H	5.617085	1.766267	3.133038
C	7.697724	2.319979	3.167026
H	8.011319	1.342944	2.795087
C	10.778343	1.374819	2.951657
H	10.063630	0.850670	2.296768
H	11.762500	1.337994	2.455231
C	9.276104	-0.014949	5.015282
C	8.620056	0.662746	6.047785
H	9.138687	1.460274	6.585571
C	7.311993	0.321544	6.391910
H	6.803655	0.867865	7.189753
C	6.659364	-0.708216	5.716323
H	5.636191	-0.978706	5.989223
C	7.315002	-1.399575	4.695392
H	6.809554	-2.215323	4.172446
C	8.619117	-1.057007	4.346550
H	9.132720	-1.613292	3.557261
C	11.750218	-1.085411	4.087274
C	11.962412	-1.491134	2.764081
H	11.680577	-0.847111	1.928218
C	12.528580	-2.737368	2.490335
H	12.685544	-3.043785	1.453228
C	12.882175	-3.590192	3.532829
H	13.321031	-4.567056	3.316467
C	12.676219	-3.192079	4.854352
H	12.960088	-3.852284	5.676729
C	12.121028	-1.946860	5.130820
H	11.971810	-1.636901	6.169521
C	14.698797	4.261467	2.152139
C	11.167701	1.196181	9.189575
N	11.080276	12.688942	9.209243
N	11.173477	9.950754	10.929916
C	10.840826	9.696857	9.829933
N	11.156138	3.918778	10.946550
C	11.532492	4.212149	9.872194
N	12.015521	4.596926	8.749270
Cu	11.697050	12.236512	11.066636
Cu	11.742220	9.392085	12.873127
Cu	10.677910	4.347038	12.921776
Cu	10.528560	1.569559	11.014744
P	10.488772	13.195592	12.768985
P	10.667783	10.626872	14.523603
P	14.003100	12.189410	11.221457
P	14.043812	9.704845	13.057701
P	8.375684	4.156237	13.159041
P	8.233173	1.696726	11.286789
P	12.058787	3.129932	14.318773
P	11.552265	0.472527	12.779273
C	11.323951	7.460644	13.001844
N	11.103315	6.313541	13.036700
C	10.916743	14.958625	13.079248
C	10.012353	15.999280	12.834426
H	9.002050	15.776114	12.485433
C	10.390869	17.325896	13.041455
H	9.672329	18.126771	12.850826
C	11.672191	17.630376	13.494926
H	11.963515	18.670061	13.661834
C	12.583329	16.600816	13.730777
H	13.595084	16.828679	14.074133
C	12.210929	15.277042	13.515420
H	12.950410	14.488404	13.680620
C	8.671044	13.236304	12.572287
C	7.799101	13.509508	13.635636
H	8.185108	13.678067	14.643510
C	6.425966	13.579760	13.420420
H	5.755819	13.786918	14.257970
C	5.909745	13.392922	12.137435
H	4.831966	13.457259	11.968135
C	6.769331	13.126968	11.074119
H	6.370319	12.980407	10.068168
C	8.145078	13.037829	11.290277
H	8.819803	12.821343	10.457329
C	10.768314	12.474832	14.449854
H	10.121889	12.958484	15.198972
H	11.810599	12.728619	14.703180
C	8.865409	10.304770	14.661807
C	8.213142	9.724493	13.568387
H	8.788431	9.460104	12.676591
C	6.841650	9.474195	13.619591
H	6.345096	9.011093	12.763633
C	6.116309	9.796308	14.765122
H	5.043040	9.595032	14.807909
C	6.763430	10.364492	15.864331
H	6.198051	10.609147	16.767253
C	8.133083	10.614183	15.815586
H	8.637012	11.042454	16.686746
C	11.273694	10.274876	16.219376
C	11.546068	8.933953	16.528726
H	11.421049	8.163008	15.762972
C	11.983425	8.578392	17.801921
H	12.193274	7.529464	18.024370
C	12.165773	9.556253	18.779856
H	12.514400	9.277347	19.777183
C	11.463993	11.250737	17.206461
H	11.265987	12.304218	16.997943
C	14.699874	13.887429	11.262344
C	14.047233	14.845054	10.471763
H	13.149229	14.562305	9.913466
C	14.524926	16.151629	10.405163
H	14.007458	16.886671	9.784317
C	15.648966	16.523710	11.142617
H	16.020694	17.550111	11.096191
C	16.292657	15.583702	11.946103
H	17.170614	15.871395	12.529823
C	15.824015	14.270693	12.004239

H	16.349062	13.550857	12.636495
C	14.906731	11.422056	9.820612
C	16.304673	11.338802	9.777064
H	16.909705	11.719573	10.604566
C	16.938642	10.782293	8.670643
H	18.029534	10.722730	8.644241
C	16.184733	10.314000	7.591980
H	16.684203	9.894392	6.715370
C	14.795917	10.400970	7.624825
H	14.197172	10.057453	6.778435
C	14.160022	10.952444	8.736723
H	13.073614	11.050867	8.754486
C	14.723660	11.398026	12.727347
H	14.400068	12.035588	13.566418
H	15.825423	11.383802	12.715865
C	15.032389	8.632149	11.943141
C	15.067850	7.009680	10.145109
H	14.526705	6.386811	9.428244
C	16.458432	6.953428	10.220371
H	17.011773	6.293540	9.547347
C	17.139573	7.726440	11.164198
H	18.229172	7.675394	11.232938
C	14.356601	7.853013	10.999524
H	13.266048	7.900720	10.947226
C	16.429406	8.555240	12.028119
H	16.966677	9.135729	12.783905
C	14.764283	9.291967	14.694298
C	15.228684	10.242034	15.610602
H	15.222640	11.306706	15.367810
C	15.717574	9.844009	16.855628
H	16.080380	10.598005	17.558277
C	15.749515	8.495137	17.199578
H	16.139306	8.186664	18.172509
C	15.279098	7.541414	16.296210
H	15.293055	6.479900	16.555610
C	14.784665	7.936640	15.057450
H	14.412606	7.179940	14.362332
C	11.908976	10.891862	18.479036
H	12.052368	11.663709	19.239246
C	7.168812	3.660993	15.712144
H	7.092634	2.603818	15.449223
C	6.730398	4.069909	16.972622
H	6.322145	3.331876	17.667333
C	6.805920	5.410627	17.341865
H	6.455899	5.728058	18.327050
C	7.326925	6.345648	16.445563
H	7.387602	7.402042	16.718559
C	7.769484	5.940121	15.189447
H	8.178990	6.683492	14.499501
C	7.438994	5.305390	12.075921
C	6.041779	5.401486	12.130025
H	5.472500	4.769682	12.817899
C	5.369985	6.314819	11.323390
H	4.279964	6.379901	11.366639
C	6.090560	7.151316	10.467122
H	5.563212	7.869928	9.834150
C	7.481357	7.073473	10.421129
H	8.051994	7.734641	9.763187
C	8.154927	6.147730	11.219752
H	9.245355	6.089879	11.196184
C	7.623082	2.495168	12.836937
H	7.983995	1.845450	13.651589
H	6.521855	2.525768	12.883034
C	7.271621	2.500924	9.946825
C	5.873476	2.417111	9.891470
H	5.323782	1.879567	10.669481
C	5.178225	2.994288	8.832668
H	4.088486	2.921682	8.794647
C	5.873942	3.648602	7.813553
H	5.333079	4.082970	6.969436
C	7.264050	3.728804	7.858007
H	7.809611	4.216710	7.046868
C	7.960584	3.160004	8.924696
H	9.051022	3.204819	8.958426
C	7.561085	-0.730550	10.154239
H	8.102158	-0.334424	9.289675
C	7.444984	0.039576	11.322357
C	6.982697	-1.993454	10.079884
H	7.070567	-2.573389	9.157736
C	6.294394	-2.514906	11.176714
H	5.838538	-3.506241	11.119377
C	6.192372	-1.766057	12.346007
H	5.659236	-2.168886	13.210415
C	6.762025	-0.493595	12.420078
H	6.657613	0.075653	13.345954
C	11.956855	3.602536	16.092992
C	10.957804	4.506524	16.469484
H	10.298721	4.927866	15.707065
C	10.800918	4.870201	17.807620
H	10.007482	5.568140	18.085275
C	11.650616	4.342237	18.777409
H	11.528304	4.623211	19.826513
C	12.661947	3.453030	18.407440
H	13.334940	3.043137	19.164583
C	12.815666	3.085403	17.073222
H	13.620073	2.398855	16.797835
C	13.850687	3.230843	13.953415
C	14.287386	4.390809	13.299252
H	13.552202	5.135260	12.978428
C	15.645796	4.597825	13.060291
H	15.973469	5.512727	12.561824
C	16.577560	3.637173	13.452252
H	17.642399	3.798438	13.265911
C	16.148924	2.466910	14.078092
H	16.872361	1.702975	14.372208
C	14.793576	2.265183	14.329674
H	14.482053	1.335226	14.809866
C	11.680904	1.320738	14.419994
H	12.357850	0.781119	15.102252
H	10.673415	1.291192	14.866702
C	13.261575	-0.105988	12.444159
C	13.992123	0.513948	11.425354
H	13.529509	1.313846	10.841716
C	15.299927	0.112136	11.153309
H	15.863700	0.608347	10.359750
C	15.881056	-0.916504	11.892455
H	16.904117	-1.234832	11.676762
C	15.153577	-1.547189	12.903800
H	15.603014	-2.362283	13.476427
C	13.847903	-1.146862	13.177295
H	13.276332	-1.659470	13.956347
C	10.689883	-1.090473	13.198702
C	10.358262	-1.487251	14.499937
H	10.601687	-0.856735	15.357724
C	9.717406	-2.706668	14.724291
H	9.467315	-3.005721	15.745148
C	9.406844	-3.542393	13.654692
H	8.908730	-4.498313	13.832903
C	9.733348	-3.153982	12.354881
H	9.486140	-3.801168	11.510567
C	10.364186	-1.935234	12.126853
H	10.609002	-1.633451	11.104140
C	7.689295	4.591658	14.805621
N	11.559061	1.189373	8.088781

C	10.796691	12.704646	8.075283	C	10.726747	9.685507	7.486710
N	11.330462	7.519836	4.278468	C	11.837545	4.195921	7.546711
C	11.577228	6.377426	4.297375				

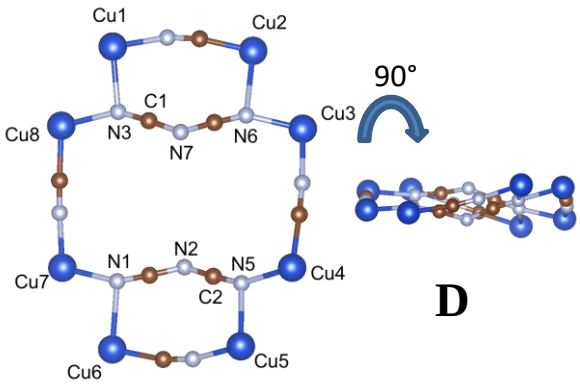

D	dist (Å)
Cu1-Cu2	5.054
Cu2-Cu3	3.372
Cu3-Cu4	5.156
Cu4-Cu5	3.370
Cu5-Cu6	5.051
Cu6-Cu7	3.430
Cu7-Cu8	5.158
Cu8-Cu1	3.409
Cu8-Cu3	8.627
Cu7-Cu4	8.593
Cu1-Cu6	10.907
Cu2-Cu5	10.731

Fig. S37. Main geometrical data of metallacycle of the DFT optimized geometry of **D**

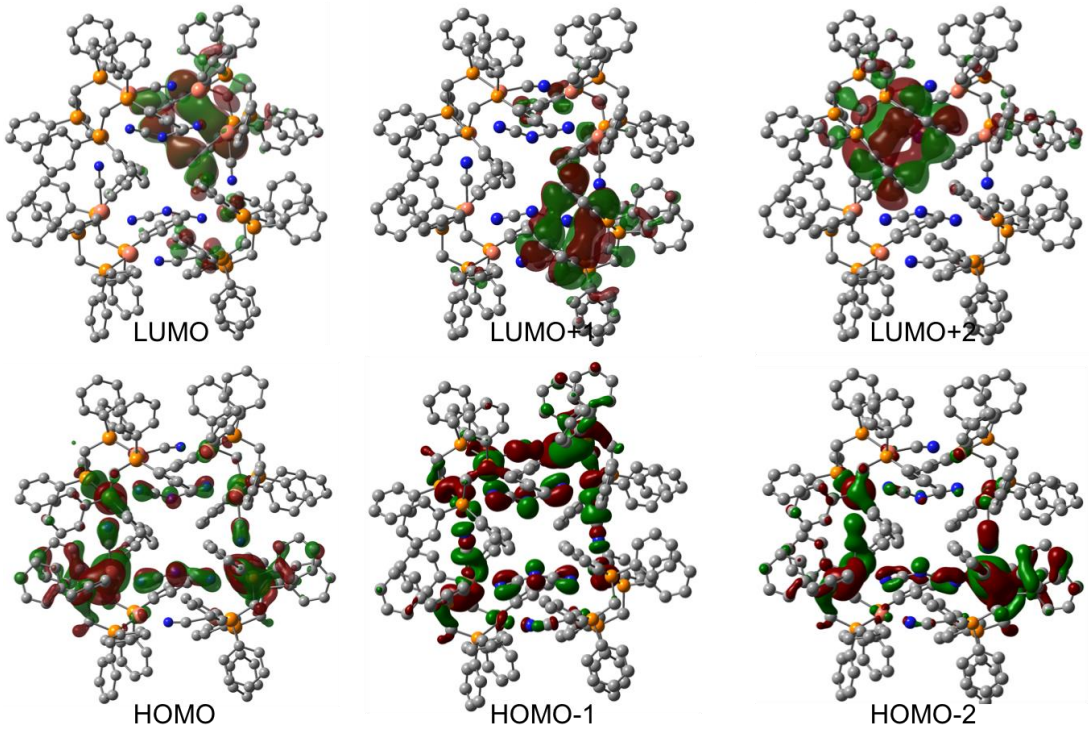

Fig. S38. Isosurface representations of the frontier molecular orbitals (MOs) of **D** (± 0.015 $(e.bohr^{-3})^{1/2}$).

Table S6. Calculated vertical electronic excited state energies of **D** and associated oscillator strength (zero for the triplet states in the absence of spin-orbit coupling consideration). The description in terms of MO transition is not given for the triplet excited states since they are numerous for each state with participation of less than 10%. The difference in the total density with S_0 is given in Fig. S40 for the description of T_1.

Singlet Excited States	Excitation Energy (eV)	λ (nm)	Oscillator Strength	Description
S_1	3.91	317	0.003	39 % HOMO → LUMO+1 35 % HOMO-2 → LUMO+1
S_2	3.98	311	0.008	51 % HOMO → LUMO+3 16 % HOMO-3 → LUMO+3 11 % HOMO-2 → LUMO+3
S_3	3.99	310	0.005	46 % HOMO-1 → LUMO 18 % HOMO-3 → LUMO 13% HOMO → LUMO
S_4	4.05	306	0.011	48 % HOMO-2 → LUMO+6 34 % HOMO → LUMO+6

Triplet Excited States	Excitation Energy (eV)	λ (nm)
T_1	3.75	330
T_2	3.78	328
T_3	3.79	327
T_4	3.80	326

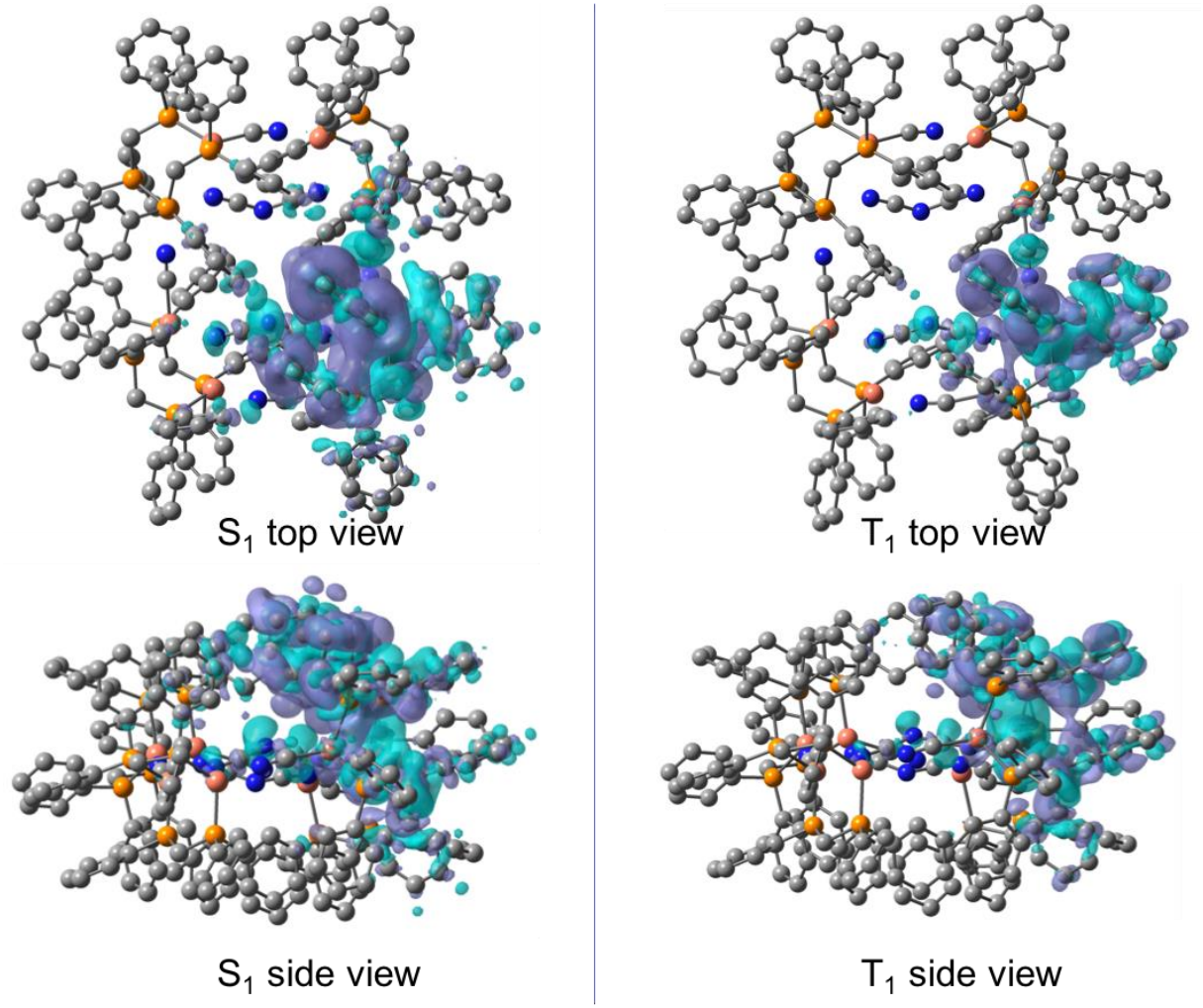

Fig S39. Isosurface representations of the electronic charge-density difference between the first vertical singlet (S_1) and triplet (T_1) excited states and the ground state (S_0) of **D** (blue = density depletion, greenish = density increase) (± 1.10^{-4} e.bohr^{-3}).

VI. EPR spectrum of the derivative F_{Cu} in the solid-state at room temperature

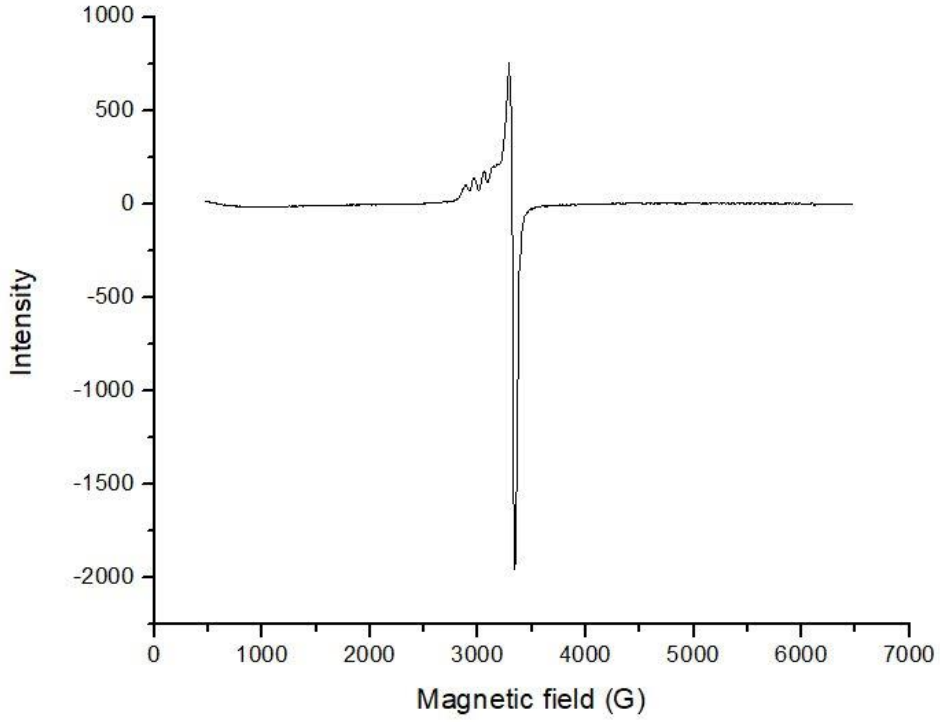

Fig S40. EPR spectrum of $\mathbf{F_{Cu}}$ recorded in the solid-state at room temperature

VII. References for the supplementary information file

[S1] M. El Sayed Moussa, S. Evariste, H.-L. Wong, L. Le Bras, C. Roiland, L. Le Polles, B. Le Guennic, K. Costuas, V. W.-W. Yam, C. Lescop, *Chem. Comm.,* **2016**, *52*, 11370-11373

[S2] M. A. Delsuc, T. E. Malliavin, *Anal. Chem.*, **1998**, *70*, 2146

[S3] D. Massiot, F. Fayon, M. Capron, I. King, S. L. Calvé, B. Alonso, J. O. Durand, B. Bujoli, Z. Gan, G. Hoatson, *Magn. Reson. Chem.* **2002**, *40*, 70–76.

[S4] H. Yersin, A. F. Rausch, R. Czerwieniec, T. Hofbeck, T. Fischer, *Coord. Chem. Rev.* **2011**, *255*, 2622.

[S5] Otwinowski, Z.; Minor, W. In *Methods in Enzymology*, (Ed.: C.W. Carter, Jr. & R.M. Sweet), New York: Academic Press**, 1997**, *276*, 307.

[S6] Altomare, A.; Burla, M. C.; Camalli, M.; Cascarano, G.; Giacovazzo, C.; Guagliardi, A.; Moliterni, A. G. G.; Polidori, G.; Spagna, R. *J. of Applied Cryst.* **1999**, *32*, 115.

[S7] Sheldrick G.M., *SHELX97,* Program for the Refinement of Crystal Structures, University of Göttingen, Germany, **1997**.

[S8] (a) Spek, A. L. *J. Appl. Crystallogr.* **2003**, *36*, 13; (b) van der Stuis, P.; Spek, A. L. *Acta Crystallogr.* **1990**, *46*, 194.

[S9] International Tables for X-ray Crystallography, vol C, Ed. Kluwer, Dordrech, **1992**.

[S10] Gaussian 16, Revision C.01, M. J. Frisch, G. W. Trucks, H. B. Schlegel, G. E. Scuseria, M. A. Robb, J. R. Cheeseman, G. Scalmani, V. Barone, G. A. Petersson, H. Nakatsuji, X. Li, M. Caricato, A. V. Marenich, J. Bloino, B. G. Janesko, R. Gomperts, B. Mennucci, H. P. Hratchian, J. V. Ortiz, A. F. Izmaylov, J. L. Sonnenberg, D. Williams-Young, F. Ding, F. Lipparini, F. Egidi, J. Goings, B. Peng, A. Petrone, T. Henderson, D. Ranasinghe, V. G. Zakrzewski, J. Gao, N. Rega, G. Zheng, W. Liang, M. Hada, M. Ehara, K. Toyota, R. Fukuda, J. Hasegawa, M. Ishida, T. Nakajima, Y. Honda, O. Kitao, H. Nakai, T. Vreven, K. Throssell, J. A. Montgomery, Jr., J. E. Peralta, F. Ogliaro, M. J. Bearpark, J. J. Heyd, E. N. Brothers, K. N. Kudin, V. N. Staroverov, T. A. Keith, R. Kobayashi, J. Normand, K. Raghavachari, A. P. Rendell, J. C. Burant, S. S. Iyengar, J. Tomasi, M. Cossi, J. M. Millam, M. Klene, C. Adamo, R. Cammi, J. W. Ochterski, R. L. Martin, K. Morokuma, O. Farkas, J. B. Foresman, and D. J. Fox, Gaussian, Inc., Wallingford CT, **2016**.

[S11] C. Adamo, V. Barone, *J. Chem. Phys.,* **1999**, 6158-69, 110.

[S12] (a) A. Schaefer, H. Horn, R. Ahlrichs, *J. Chem. Phys.*, **1992**, *97*, 2571-2577; (b) A. Schaefer, C. Huber, R. Ahlrichs, *J. Chem. Phys*., **1994**, *100*, 5829.